ACS Photonics

Review

pubs.acs.org/journal/apchd5

Magnetoplasmonics and Femtosecond Optomagnetism at the Nanoscale

D. Bossini,[*,†] V. I. Belotelov,[‡,§] A. K. Zvezdin,[‡,∥,⊥,#] A. N. Kalish,[‡,§] and A. V. Kimel[#,¶]

[†]Institute for Photon Science and Technology Graduate School of Science, The University of Tokyo, 7-3-1 Hongo, Bunkyo-ku, Tokyo 113-0033, Japan

[‡]Russian Quantum Center, 100 Novaya Street, Skolkovo, Moscow Region 143025, Russia

[§]Faculty of Physics, Lomonosov Moscow State University, Leninskie Gory, Moscow 119991, Russia

[∥]Prokhorov General Physics Institute RAS, 38 Vavilov Street, Moscow 119991, Russia

[⊥]Moscow Institute of Physics and Technology, 9 Institutskiy Per., Dolgoprudny, Moscow Region 141700, Russia

[#]Moscow State Technical University of Radio Engineering, Electronics and Automation, Moscow 119454, Russia

[¶]Institute for Molecules and Materials, Radboud University, Heyendaalseweg 135, Nijmegen, The Netherlands

ABSTRACT: The reciprocal interaction between spins and light has long been one of the main topics in fundamental studies of magnetism. Recent developments of nanolitography and other experimental approaches have disclosed that the interaction of light with magnetic nanostructures is qualitatively different from the regime in which the size of the illuminated media is much larger than the wavelength. In particular, the subwavelength regime of light−spin interaction revealed the plasmon-mediated enhancement and emergence of new magneto-optical phenomena. Novel possibilities of optical control of magnetism on the nanometer scale via plasmonic resonances have emerged as well. Moreover, it was shown that femtosecond laser pulses are able to generate magnons with nanometer wavelengths and with wavevectors near the edges of the Brillioun zone. The use of optical radiation to either excite ultrafast spin dynamics or detect the magnetic properties of structures at the nanoscale began a new chapter in the fascinating story of the human discovery of magnetism. This review aims at summarizing recent advances in magnetoplasmonics and optomagnetism at the nanoscale.

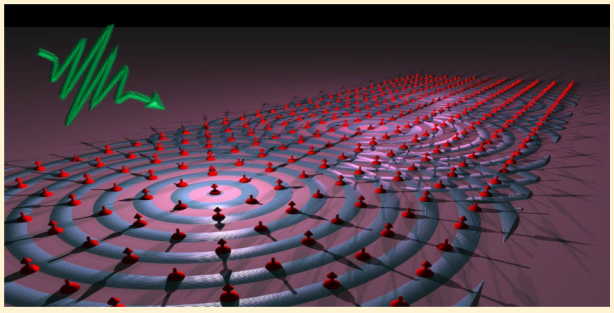

KEYWORDS: *magnetism, magneto-optics, ultrafast spectroscopy, optomagnetism, nanoscale*

Can light interact with spins and control them? The magneto-optical Faraday effect discovered in 1845 played a crucial role in unraveling the electromagnetic nature of light. Today the magneto-optical Faraday, Kerr, Cotton−Mouton, and Voigt effects are powerful means to probe the magnetic state of media.[1] In all these phenomena either the polarization or the intensity of polarized light is modified upon the interaction with magnetically ordered or magnetized materials. Phenomenologically these effects can be described in terms of spin-dependent contributions to the dielectric permittivity tensor. Interestingly, the very same terms can be responsible for inverse optomagnetic Faraday, Kerr, and Cotton−Mouton effects when the magnetic configuration of a medium is manipulated via the interaction with polarized light.[2,3] Experiments with femtosecond laser pulses have shown that optomagnetism is a unique stimulus in contemporary magnetism. In particular, it allows the generation of femtosecond effective magnetic field pulses with intensities up to several tesla,[4] the control of coherent motion of spins,[3] and steering magnetic phase transitions.[5,6] It has been suggested that if the optomagnetic approach could be mastered at the nanoscale, such an optical control of magnetism could be employed in future magnetic-recording and information-processing technologies. Scientists have already succeeded in concentrating light energy in an area of subwavelength size by employing a plasmonic nanostructure.[7] However, it was also realized that the understanding of magneto-optics and optomagnetism at the nanoscale is not trivial at all. Some conventional approximations, such as the continuous medium approximation and the assumption of homogeneous field, cannot describe this regime of light−matter interaction.

In this review we aim to recall recent progress in the closely related areas of magneto-optics and optical control of magnetism at the nanoscale. The review is organized as follows. First, we present the magneto-optical effects employed in the investigation of nanostructures. The pivotal concept of plasmonic resonance is introduced: it plays a key role in

Special Issue: Nonlinear and Ultrafast Nanophotonics

Received: February 15, 2016
Published: June 1, 2016

DOI: 10.1021/acsphotonics.6b00107
ACS Photonics 2016, 3, 1385−1400

magnifying the magneto-optical response of nanostructured materials, and it even allows the observation of novel effects. Then, we provide a summary of the experimental developments at the nanoscale of the three major research directions in the ultrafast spin dynamics area: the ultrafast demagnetization of metallic ferromagnets, the picosecond all-optical switching of the magnetization in ferrimagnetic metallic alloys, and the excitation and manipulation of coherent spin waves in dielectric materials. An argument based on the dielectric tensor is given, revealing the intrinsic deep link between magneto-optical effects (discussed in the first part of the review), Raman scattering on magnons, and optomagnetism. Subsequently we recall the concept of plasmonic resonance, by reporting how it has been employed to increase the efficiency of the ultrafast demagnetization and switching processes.

MAGNETO-OPTICS AT THE NANOSCALE

Magneto-optical effects provide a way for light control and modulation at GHz and THz frequency ranges that is of prime importance for modern telecommunication and microwave photonics. In addition to that, magneto-optical effects could be used for magnetic field sensors and visualizers as well as for bio- and chemosensors. However, usually a magnetic field provides only minor modulations of the light intensity or polarization measured by some fraction of a percent. This is the main constraint that has hampered the role of magneto-optics in applied nanophotonics so far. Therefore, it is essential to seek strategies to enhance magneto-optical effects, for which there are several ways. While the potential of methods relying purely on material synthesis has been already extensively explored, nanostructuring is very promising for tailoring the optical properties of materials.[8] This approach reflects a new paradigm of modern optics in which optical properties are mainly determined by geometrical resonances rather than by electronic ones. Examples of a fruitful magneto-optical implementation of this approach are magnetophotonic crystals and magnetic nanoresonators, providing a considerable enhancement of the Faraday effect.[9−12]

MAGNETOPLASMONICS

The other rather interesting approach to boost magneto-optical effects involves surface plasmon polaritons (SPPs), coupled oscillations of the electromagnetic field and the electron plasma in a metal that are localized and propagate along a metal/dielectric interface.[13] Nowadays, the field of plasmonics represents an exciting new area for the application of surface plasmons in which surface-plasmon-based circuits merge the fields of photonics and electronics at the nanoscale.[14] Indeed, SPPs can serve as a basis for constructing nanoscale photonic circuits that will be able to carry optical signals and electric currents.[15] When an incident light beam is coupled to SPPs inside a magnetic medium and then reemitted back to the optical far field, its properties become significantly more sensitive to the medium permittivity and magnetization. Here we consider plasmonic structures containing magneto-optical materials and discuss the current state of the art in this area.

The frequency of collective plasma oscillations, i.e., the plasma frequency, in a free electron gas is $\omega_p = (ne^2/m)^{1/2}$ (in SI units), where n is an equilibrium density and e and m are electron charge and mass, respectively. In the presence of a planar interface between a plasma medium of permittivity ε_1 and a nonconducting medium of permittivity ε_2 a surface plasmon mode appears. Its frequency is lower than that of the bulk plasma: $\omega_s = \omega_p/\sqrt{1+\varepsilon_2}$. If the phase speed of the surface plasmon is compared with the speed of light, it can be coupled with an electromagnetic field, thus originating the SPP mode. An SPP is a transverse magnetic polarization (TM)-polarized wave. The dispersion of the SPP mode is given by

$$\beta = k_0\sqrt{\frac{\varepsilon_1\varepsilon_2}{\varepsilon_1+\varepsilon_2}} \tag{1}$$

where k_0 is the vacuum wavenumber.

It is important to note that the wavenumber of a free electromagnetic wave inside the dielectric, given by $k_0\sqrt{\varepsilon_2}$, is smaller than the SPP wavenumber at the metal/dielectric interface by a factor $\sqrt{\varepsilon_1/(\varepsilon_1+\varepsilon_2)} > 1$. It prevents a direct coupling of light to the SPP mode. That is why some special experimental arrangements have been designed for a successful SPP excitation. The photon and SPP wavevectors can be matched by using either photon tunneling in the total internal reflection geometry (Kretschmann and Otto configurations) or diffraction effects. In the latter case either a metal or a dielectric is periodically perforated by a slit or hole array, and the structures can be referred to as *plasmonic crystals*.

Plasmonic crystals allow tailoring the dispersion of SPPs in a desired way and the concentration of electromagnetic energy in a small volume near the metal/dielectric interface. The latter was shown recently to have a great potential for ultrafast nanophotonics since it allows switching permittivity of gold by a short laser pulse on a time-scale of several hundreds of femtoseconds.[16]

If a plasmonic crystal contains a magnetic material, it can be addressed as a magnetoplasmonic crystal. The typical example is a smooth magnetic dielectric film with a metallic grating placed on top.

Magneto-optical effects can be classified as polarization and intensity effects. A well-known representative of the polarization effects is the magneto-optical Faraday effect, manifesting itself in a rotation of the polarization plane of a linearly polarized beam at an angle when it propagates along the medium magnetization **M**. If light propagates perpendicular to the medium magnetization, then the Cotton−Mouton or Voigt effect arises.[17] A linearly polarized light having its polarization plane oriented at an angle to the magnetization direction becomes elliptically polarized after propagation through the medium.

On the other hand, the transverse magneto-optical Kerr effect (TMOKE) is an intensity effect. The TMOKE may be observed only in absorbing materials if the magnetization lies in the sample plane but is perpendicular to the light incidence plane. For the p-polarization of the incident beam (polarized in the incident plane) it is measured by the relative change in the reflected light intensity when the medium is remagnetized:

$$\delta_p = \frac{I(\mathbf{M}) - I(-\mathbf{M})}{I(0)} \tag{2}$$

where $I(\mathbf{M})$ and $I(0)$ are the intensities of the reflected light in the magnetized and nonmagnetized states, respectively. Both the Faraday effect and the TMOKE are linear in the magnetization.

DOI: 10.1021/acsphotonics.6b00107
ACS Photonics 2016, 3, 1385−1400

PLASMONIC ENHANCEMENT OF THE TRANSVERSE KERR EFFECT

Early investigations on the interplay between SPPs and magneto-optics addressed SPPs propagating along the smooth surface of a ferromagnetic film[18−20] or along a smooth semiconductor surface in an external magnetic field.[21,22] In that case, the magnetic field modifies the SPP wave vector but leaves its transverse magnetic polarization unchanged. The SPP-assisted increase of the TMOKE was reported. This increase is due to the shift of a SPP resonance in a transverse magnetic field. The shift happens only for propagating SPPs. The resonance frequency of the localized SPPs is hardly influenced by the magnetic field, and, consequently, no pronounced changes in the TMOKE at localized plasmonic resonances are observed. Nevertheless, the interaction of localized and propagating surface plasmon modes modifies the SPP dispersion and thus the TMOKE signal.[23] In addition to that, localized SPPs can also influence the second-harmonic TMOKE, which was experimentally shown.[24,25]

Vast research was performed on bimetallic systems containing both noble and ferromagnetic metals. For example, the presence of a noble metal spacer with a typical thickness of several tens of nanometers leads to the separation of the plasmonic and magnetic interfaces. It allows the SPPs to propagate for a rather long distance along the air and noble metal interface, so the TMOKE results increased by several times.[26−29] In this scheme, Au/Co/Au trilayers are utilized.[30,31] Structured all-metallic plasmonic systems were studied as well, such as perforated Au/Co multilayers.[32,33] A resonant increase of the TMOKE was reported for metallic gratings made of Co, Fe, or Ni.[34,35] Plasmonic crystals containing hybrid noble-metal/ferromagnetic-metal multilayers were designed for magnetic modulation of the SPP wavenumber.[36,37] Nonlinear TMOKE was also detected in Au/Co/Ag multilayers.[38] Since the overall optical losses for such systems are lower than in the case of pure ferromagnetic metals, the increase of the TMOKE resonance due to propagating SPPs in these structures is even more pronounced. However, the presence of the ferromagnetic metals still provides relatively high losses. Pure noble metal structures also provide enhancement of the TMOKE,[39] due to the Lorentz force acting on free electrons in a magnetic field. The required external magnetic field is as high as several tesla.

The necessary condition for the TMOKE occurrence is $[\mathbf{k} \times \mathbf{N}] \neq 0$ where $\mathbf{k}$ is the wave vector and $\mathbf{N}$ is the vector normal to the metal−dielectric interface. Moreover, the cross product $[\mathbf{M} \times \mathbf{N}]$ is also very important. It is nonzero near the surface of the magnetized film. The magnetic field breaks the symmetry with respect to time reversal, while the interface (and the $\mathbf{N}$ vector normal to it) breaks the space inversion. Interestingly, space−time symmetry breaking is characteristic of media with a toroidal moment τ which has transformation properties similar to those of $[\mathbf{M} \times \mathbf{N}]$.[40] Consequently, the problem of the SPP propagation along the interface of a transversely magnetized medium is similar to that of electromagnetic waves propagating in a bulk medium with a toroidal moment parallel to this direction. In electrodynamics, a toroidal moment is known to give rise to optical nonreciprocity as manifested by the difference between the wave vectors for waves propagating forward and backward with respect to the toroidal moment.[41,42] Thus, the magneto-optical nonreciprocity is always present for the transverse configuration and reveals itself, for example, in the properties of magnetic plasmon-solitons.[43]

It follows from Maxwell's equations that, in contrast to all other possible magnetization directions, the transverse magnetization does not change the polarization state of the SPP but only changes its wavenumber κ:[44]

$$\kappa = \kappa_0(1 + \alpha g) \tag{3}$$

where $\kappa_0 = k_0\left(\frac{\varepsilon_1\varepsilon_2}{(\varepsilon_1+\varepsilon_2)}\right)^{1/2}$ and $\alpha = (-\varepsilon_1\varepsilon_2)^{-1/2}(1-\varepsilon_2^2/\varepsilon_1^2)^{-1}$, ε_1 and ε_2 are dielectric constants for metal and dielectric, respectively, and gyration g is the parameter linear in the magnetization that is responsible for magneto-optical properties of a material (in terms of the dielectric tensor, $g = i\varepsilon_{zx} = -i\varepsilon_{xz}$ if the magnetization is directed along the y-axis). It follows from eq 3 that, in the first approximation, the wavenumber of the surface wave depends linearly on the film gyration g.

In a magnetoplasmonic crystal in which the metallic layer is perforated by an array of parallel slits and the dielectric layer is magnetized along the slits (Figure 1a), the plasmon reflection

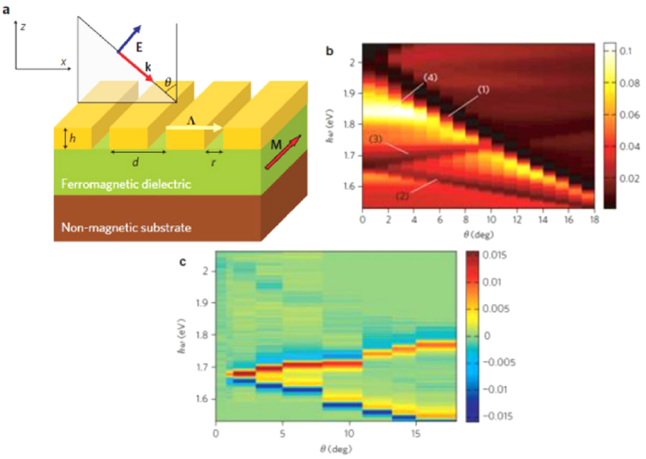

Figure 1. Light modulation in a magnetoplasmonic crystal by a transverse magnetic field. (a) Magnetoplasmonic crystal of a gold grating and a ferromagnetic dielectric illuminated with incident p-polarized light. (b, c) False-color plots showing the experimentally measured transmission (b) and the TMOKE parameter δ_T (c) as a function of photon energy (vertical axis) and the angle of incidence (horizontal axis). The geometrical parameters are grating height h = 120 nm, grating period d = 595 nm, and grating slit width r = 110 nm. The in-plane magnetic field strength is 200 mT. The features labeled 1−4 are related to the SPPs or Fabry−Perot eigenmodes.[51]

and transmission resonances are shifted in frequency depending on the magnitude and direction of the field virtually without changing their shape, which leads to an enhancement of the TMOKE.[45]

The most pronounced TMOKE enhancement takes place for high-quality resonances that are achieved if the ferromagnetic metal is substituted by a low absorptive noble one and the dielectric layer is magnetized. Probably, the best candidates for magnetic dielectrics are bismuth rare-earth iron garnet films of composition $Bi_xR_{3-x}Fe_5O_{12}$, where R is a rare-earth element.[46] Their blue band gap has an energy equal to 2.7 eV, and, although there are electronic transitions in Fe^{3+} ions in the range 1.3−2.7 eV, the films are sufficiently transparent in the visible and near-infrared range. Bi ions enhance the magneto-optical response of the iron garnets, thus providing a specific Faraday rotation of several degrees per micrometer and even larger at moderate optical losses. Iron garnets serve as efficient

DOI: 10.1021/acsphotonics.6b00107
ACS Photonics 2016, 3, 1385−1400

magneto-optically active layers of the photonic crystals for light intensity modulators and magnetic sensors.[47,48] On the other hand, iron garnet thin films are being used quite successively in experiments on spin−orbit torque transfer and nonlinear spin-wave dynamics.[49,50]

Incorporating iron garnets in the magnetoplasmonic crystal allows observing the giant TMOKE in the magnetoplasmonic crystals in transmission. In detail, the magnetic part of the magnetoplasmonic structure is a 2.5 μm thick bismuth-substituted rare-earth iron garnet film of composition $Bi_{0.4}(YGdSmCa)_{2.6}(FeGeSi)_5O_{12}$, grown on a gadolinium gallium garnet, $Gd_3Ga_5O_{12}$, substrate with (111) orientation. The film possesses uniaxial magnetic anisotropy in the direction perpendicular to the film plane. The magnetoplasmonic structure sample shown in Figure 1a was fabricated by thermal deposition of a gold layer on the bismuth-substituted rare-earth iron garnet film and subsequent electron beam lithography combined with reactive ion etching in Ar plasma.

Results of the experimentally measured zero-order transmission for the configuration shown in Figure 1a are presented in Figure 1b.[51] The pronounced Fano resonances 1 in Figure 1b can be attributed to the SPP at the air/gold interface, while the Fano resonances 2 and 3 are related to the SPPs at the gold/magnetic-film interface. Finally, the prominent transmission peak 4 is attributed to the collective Fabry−Perot cavity mode inside the slits.

The experimentally measured TMOKE parameter δ is defined in accordance with eq 2, with I being the transmission coefficient (Figure 1c). To ensure that the sample magnetization is oriented almost completely in the plane, a relatively large external magnetic field of 200 mT was applied. Outside of the resonances the absolute value of δ is very small. Actually in this case, δ cannot be measured experimentally, which means that it is below 10^{-3}. With this background, pronounced positive (brighter) and negative (darker) peaks are observed in which δ reaches 1.5×10^{-2}, demonstrating a TMOKE increase by at least 1 order of magnitude. Electromagnetic modeling for the nonresonant case gives $\delta = 8 \times 10^{-4}$, implying an enhancement factor of about 20. Compared to the uncovered bare iron garnet film, the enhancement factor is much larger, by about 10^3. From these results we can claim that a giant TMOKE has been observed in transmission. It should be noted that here we use a magnetic film with a relatively small concentration of bismuth. For iron garnets with a composition $Bi_3Fe_5O_{12}$ the specific Faraday rotation is about 6° at λ = 630 nm, 13 times larger than for our sample.[1] Since the δ-value is proportional to the gyration (and to the specific Faraday rotation), δ should be also 13 times larger than the one observed in our experiments; that is, δ may exceed 0.2 by choosing the right concentration of bismuth.

The regions of the enhanced TMOKE clearly correspond to the regions of SPP excitation at the gold/ferromagnet interface (compare Figure 1b and c). No notable TMOKE increase is observed for other resonant regions, in agreement with the discussion above. This highlights the TMOKE's sensitivity to the excitation of different eigenmodes.

The optimization of the plasmonic crystal structure along with the excitation of the hybrid modes—waveguide-plasmon polaritons formed by coupling particle plasmons with a planar photonic waveguide—provided recently a further increase of the TMOKE up to 15%.[52,53]

A sophisticated multilayer structure consisting of a magneto-photonic crystal with a rare-earth iron garnet microresonator layer and a plasmonic grating deposited on it was fabricated and studied in order to combine functionalities of photonic and plasmonic crystals (Figure 2).[54] The plasmonic pattern also

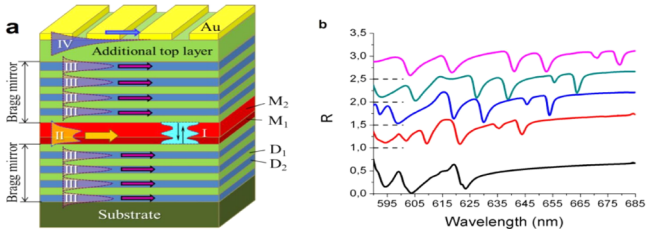

Figure 2. (a) Schematic of the photonic magnetoplasmonic sample. The layers D_1 are SiO_2 (thicknesses are 117 nm for the stack layers and 100 nm for the top layer), the D_2 layers are TiO_2 (76 nm thick), layers M_1 and M_2 are magnetic dielectrics of composition $Bi_{1.0}Y_{0.5}Gd_{1.5}Fe_{4.2}Al_{0.8}O_{12}$ and $Bi_{2.8}Y_{0.2}Fe_5O_{12}$, respectively (the thicknesses are 72 and 271 nm, respectively), and the bars on top depict the gold grating (height h_{Au} = 60 nm, period d = 370 nm, slit width w_{slit} = 220 nm). Filled curves represent schematically the eigenmode profiles in the structure, and the arrows show the wavevectors β for corresponding modes: a Fabry−Perot microresonator mode (I), a waveguide mode of the microresonator magnetic layer sandwiched between two Bragg mirrors (II), a waveguide mode localized in the higher refractive index layers of the Bragg mirrors (III), a surface plasmon-polariton at the gold/dielectric interface (IV). (b) Angular dispersion of the optical resonances experimentally measured in the reflectivity geometry for TM-polarized incident light. Incidence angles (from bottom to top): 0°, 4°, 6°, 8°, 10°. The spectra are shifted vertically by 0.5.[54]

allows the excitation of the hybrid plasmonic-waveguide modes localized in dielectric Bragg mirrors of the magnetophotonic crystal or waveguide modes inside its microresonator layer. These modes give rise to additional resonances in the optical spectra of the structure and to the enhancement of the TMOKE.

FARADAY EFFECT IN MAGNETOPLASMONIC CRYSTALS

If the magnetoplasmonic crystal is magnetized perpendicular to the sample's plane or in-plane but along the direction of the SPPs or waveguide mode propagation, then the magneto-optical effects of polarization rotation arise. These are the Faraday effect and the polar and the longitudinal Kerr effects.

Polarization effects in plasmonic structures have been intensively studied. Two-dimensional (2D) plasmonic crystals were considered, such as perforated Co films.[55] Great attention was given to bimetallic structures, typically containing Au and Co. In particular, the Faraday effect was studied in 2D plasmonic crystals made of a perforated Au/Co/Au multilayer.[56] An enhancement of the Kerr rotation due to localized SPPs was found in several systems such as Ni nanowires,[57] Au/Co/Au nanosandwiches,[58−60] and ferrimagnetic garnet films incorporating Au particles.[61−64]

At the nonresonant frequencies the Faraday rotation is close to that of a single magnetic film and is defined by the film's thickness. At the eigenmodes' excitation the resonant features of the magneto-optical response are expected. The essential eigenmodes for the magneto-optical activity are the surface plasmon polariton at the metal/dielectric interface and the waveguide modes of the dielectric layer.

The Faraday rotation can be considered qualitatively as a result of conversion of TE−TM field components. Two

DOI: 10.1021/acsphotonics.6b00107
ACS Photonics 2016, 3, 1385−1400

mechanisms for the resonant behavior of the Faraday effect are possible. Let the incident wave be p-polarized. First, at the frequency ω_{TM}, favorable for the TM mode or the SPP excitation, it partly converts to the TE mode. But since the excitation condition for the TE mode is not fulfilled, it originates from the structure contributing to the far field. The enhancement of the Faraday effect is due to the fact that the effective path of the TM mode or the SPP is larger than in the nonresonant case. Second, at the frequency ω_{TE} the TM wave comes from the structure partly converting to the TE mode. At this, the TE mode has a large effective path that causes the enhancement of the Faraday effect. Thus, the mechanism of the Faraday rotation enhancement depends on the type of excited eigenmode.

If the magnetic film thickness is comparable to the wavelength, the waveguide modes become essential.[65,66] As shown in Figure 3 the Faraday rotation demonstrates both

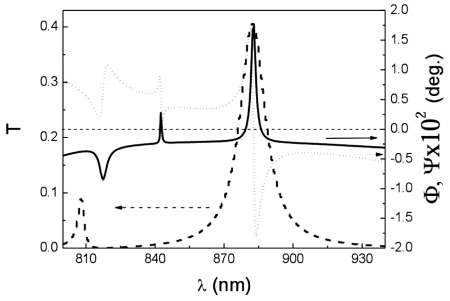

Figure 3. Spectra of the optical transmittance (dashed line), the Faraday rotation (solid line), and the ellipticity (dotted line) of the magnetoplasmonic crystal of the Au grating of thickness 65 nm and uniform bismuth iron garnet film of thickness 535 nm; d = 750 nm, r = 75 nm (see Figure 1a). The dielectric is magnetized perpendicular to the sample plane. The permittivity of the substrate is equal to 1.[65,66]

negative and positive peaks. Furthermore, the positive Faraday rotation peak at λ = 883 nm corresponds to more than 4 times enhancement, being compared to the single magnetic layer of the same thickness placed in an optically matched surrounding medium that exhibits a Faraday angle of −0.47°. In addition to that, the positive Faraday rotation peak coincides with the resonance in transmission, allowing about 40% of the incident energy flux to be transmitted. At the same time, the negative Faraday maximum at λ = 818 nm corresponds to almost negligible transmission. The peaks of the Faraday angle are accompanied by the abrupt changes of the light ellipticity. However, the ellipticity becomes zero at the resonance wavelength, and the transmitted light remains linearly polarized, but with substantial rotation of the polarization plane.

In refs 44 and 67 it was emphasized that the Faraday rotation in periodic systems is strongly related to the group velocity and shows its maximum values if v_g is vanishing. In the case of magnetic photonic crystals this dependence for the specific Faraday angle can be written as

$$\Phi_{sp} = \langle Q \rangle \frac{\omega}{2V_g} \tag{4}$$

where $\langle Q \rangle$ is the matrix element of the magneto-optical parameter $Q = g/\varepsilon$ calculated in the volume of the single lattice cell of the system. eq 4 demonstrates the strong correlation between the Faraday effect enhancement and reduction of v_g. In the case of plasmonic crystals the mechanism is similar. At normal incidence the eigenmodes are excited at the Γ point of the Brillouin zone, corresponding to the band gap edges. At this, the excited modes experience a decrease of the group velocity, while the effective time of the interaction of a mode with the magnetic media and the conversion to the opposite mode increase. So the Faraday effect is enhanced.

The experimental demonstration of the Faraday effect enhancement in the plasmonic crystals similar to the one considered above was reported in ref 68. Three samples were fabricated with different grating periods, namely, 400, 450, and 495 nm. The grating was formed by 120 nm wide and 65 nm thick nanowires placed on top of a 150 nm thick bismuth iron garnet film. A magnetic field of 140 mT was applied normally to the magnetic film, and the Faraday rotation was measured shining a TM-polarized optical beam at normal incidence. The Faraday rotation of the plasmonic photonic crystals compared with that of the bare magnetic film is shown in Figure 4a.

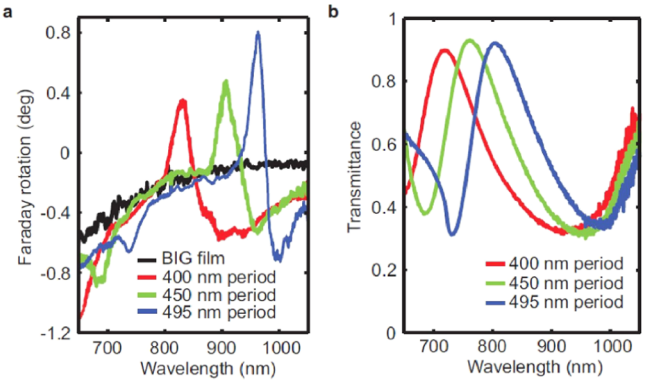

Figure 4. Faraday rotation and transmittance measured through a magnetoplasmonic crystal. (a) Faraday rotation of the three samples measured at normal incidence (TM polarization), compared with the Faraday rotation of the bare iron garnet film. (b) Transmittance of the three samples measured at normal incidence (TM polarization).[68]

The spectra of the Faraday rotation exhibit resonant features. The sample of 495 nm period displays a maximum Faraday rotation of 0.80° at λ = 963 nm, which is an 8.9 times enhancement of the −0.09° Faraday rotation of the bare iron garnet film. As seen from Figure 4a and b, the 495 nm period sample shows 36% transmittance at λ = 963 nm. In comparison, the sample of 450 nm period exhibits a Faraday rotation of 0.45° at λ = 907 nm. Compared to −0.11° Faraday rotation of the bare magnetic film, it is enhanced by 4.1 times.

NOVEL MAGNETO-OPTICAL INTENSITY EFFECT IN PLASMONIC CRYSTALS

As we have discussed so far, the implementation of the nanostructured hybrid materials provides a remarkable increase of the TMOKE and the Faraday effect. Interestingly, plasmonic structures can give origin to novel magneto-optical phenomena as well.[69,70] In particular, the plasmonic crystal consisting of a one-dimensional gold grating on top of a magnetic waveguide layer allows a magneto-optical intensity effect in the longitudinal configuration (i.e., a magnetic field is applied in the plane of the magnetic film and perpendicular to the slits in the gold grating). The longitudinal magnetization of the structure modifies the field distribution of the optical modes and thus changes the conditions of the mode excitation. In the optical far-field, this manifests in the alteration of the optical

DOI: 10.1021/acsphotonics.6b00107
ACS Photonics 2016, 3, 1385−1400

transmittance or reflectivity when the structure becomes magnetized. Thus, this effect is described similarly to the TMOKE by a relative change of the blue transmittance or reflectance (see eq 2), but in this case one should compare demagnetized and longitudinally magnetized states. Such a magneto-optical effect represents a novel class of phenomena related to the magnetic field induced modification of the Bloch modes of the periodic hybrid structure. Therefore, we define it as *the longitudinal magneto-photonic intensity effect* (LMPIE).

In the longitudinal magnetic field the two principal modes of the magnetic layer—TM and TE modes—acquire additional field components and thus turn into quasi-TM and quasi-TE modes, respectively[71] (Figure 5). Thus, the coupling between the TE and TM field components emerges in the magnetized layer. This lies at the origin of the LMPIE.

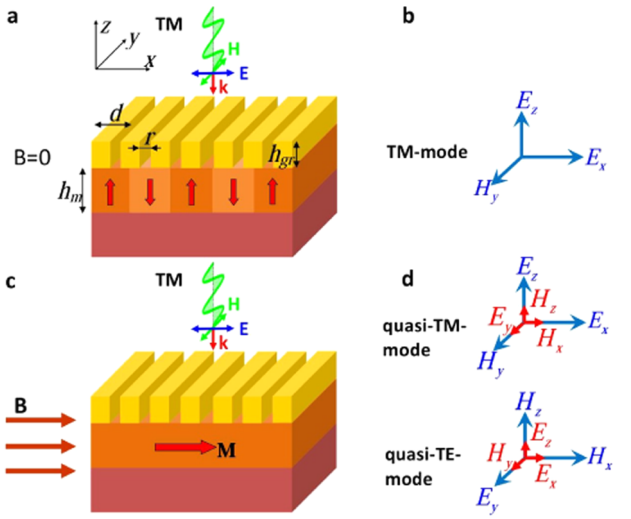

Figure 5. Electromagnetic modes of the magnetoplasmonic crystal. (a, c) Schematics of magnetoplasmonic crystals in (a) demagnetized (multidomain) and (c) longitudinally magnetized conditions. The magnetoplasmonic crystal consists of a gold grating of height h_{gr} stacked on a smooth ferromagnetic dielectric of thickness h_m grown on a nonmagnetic substrate. The gold grating has period d and slit width r. (b, d) Optical modes that can be excited by incident TM-polarized light for the (b) demagnetized and (d) longitudinally magnetized structure. The long blue arrows represent the principal field components associated with TM and TE modes in the nonmagnetic case, while the short red arrows indicate the components induced by the longitudinal magnetization.[69]

Let us discuss this configuration in detail and first consider a demagnetized plasmonic crystal illuminated by linearly polarized light, with the electric field vector perpendicular to the slits and parallel to the plane of the mode propagation. Only TM modes are excited in the dielectric layer at some frequencies ω_{TM}. At one of the TE mode's eigenfrequencies ω_{TE}, no waveguiding takes place and reflection/transmission spectra generally have no peculiarities at around ω_{TE}. However, if the plasmonic crystal is magnetized, then a waveguide mode can be excited at the frequency near ω_{TE}, as the quasi-TE mode has nonzero TM components. This leads to the redistribution of transmitted, reflected, and absorbed energy, and the spectrum should acquire a resonant feature, namely a dip. The value of the transmission dip depends on g. Consequently, at around ω_{TE} one should expect a kind of intensity magneto-optical effect expressed as $\delta = (T_0 - T_M)/T_0$, where T_M and T_0 are the transmission coefficients of the magnetized and nonmagnetized structures, respectively.

The experimental demonstration of the LMPIE was performed for a magnetoplasmonic crystal based on a 1270 nm thick magnetic film of composition $Bi_{2.97}Er_{0.03}Fe_4Al_{0.5}Ga_{0.5}O_{12}$, possessing a large real part of gyration $g = 0.015$ and an absorption coefficient $\alpha = 400$ cm^{-1} at 840 nm.[69] The other prominent feature of this sample is that it was designed such that the dispersion curves of the principal TM and TE modes corresponding to $m = 2$ intersect at the Γ point ($\kappa = 0$) of the Brillouin zone. As a consequence both modes can be excited by normally incident light of the same frequency. The LMPIE was observed in the transmission geometry. No intensity modulation occurs for the bare magnetic film (Figure 6a, green curve). The longitudinally

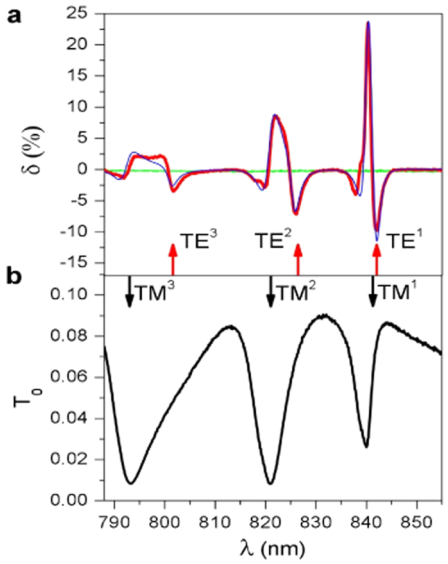

Figure 6. Magnetophotonic effect measured via the intensity modulation induced by magnetizing the magnetoplasmonic crystal. (a) Spectrum of the LMPIE when a magnetic field $B = 320$ mT reaching almost the saturation value is applied. The blue curve shows the calculated values of δ. There is no LMPIE for the bare magnetic film (green curve). (b) Spectrum of the optical transmittance for the demagnetized structure. Black and red arrows indicate calculated spectral positions of the quasi-TM and quasi-TE resonances, respectively. The modes are denoted by the number of their H_y or E_y field maxima along the z-axis. The light beam is TM-polarized, and it is incident on the sample at normal incidence. The sample parameters are $d = 661$ nm, $h_{gr} = 67$ nm, $r = 145$ nm, and $h_m = 1270$ nm (see Figure 5).[69]

applied magnetic field resonantly increases the transmittance by 24% at $\lambda = 840$ nm (Figure 6a). There are also resonances at about 825 and 801 nm, although their values are several times smaller.

The transmittance spectrum demonstrates three Fano resonances clearly related to the excitation of quasi-TM modes whose calculated spectral positions are shown by the black arrows in Figure 6b. The calculated wavelengths of the quasi-TE modes indicated by the red arrows in Figure 6a, on the other hand, confirm that the excitation of these modes is responsible for the LMPIE peaks. A longitudinal magnetic field causes almost no shift of the Fano resonances but modifies their shapes substantially. That is why the LMPIE spectral lines have rather complex multiple-peak character. An important

DOI: 10.1021/acsphotonics.6b00107
ACS Photonics 2016, 3, 1385−1400

feature of the designed sample is that the TE-mode resonance is tuned away from the transmittance minimum, allowing one to simultaneously have high transmittance (see, for example, the negative peak of $\delta = -10.3\%$ at $\lambda = 842$ nm in Figure 6a).

The LMPIE shows maximum values of about 24% at $\lambda = 840$ nm where both quasi-TE and quasi-TM mode resonances are excited. A simultaneous excitation of the two orthogonal modes allows more efficient trapping of the TM-polarized illumination and its conversion into the quasi-TE mode due to the applied magnetic field.

The measured magnetophotonic intensity effect with 24% modulation can be considered giant since it is a second-order effect in g (as it is an even function of the magnetic field). The modulation level can be increased even further by using materials with better magneto-optical quality, manifesting the relevance of the LMPIE for applications in modern telecommunication devices. On the other hand, the effect of mode switching is of great potential for active plasmonics and metamaterials.[72,73] For example, it might be used in optical transistors to allow efficient control of light propagation in magnetic waveguides through nonlinear interaction[74] with the excited modes of the magnetoplasmonic crystal.

FEMTOSECOND OPTOMAGNETISM: BASIC CONCEPTS AND NANOSCALE DYNAMICS

The study of the interaction between femtosecond laser pulses and magnetically ordered materials is the essence of the *ultrafast optomagnetism* research field. In the digital information era the demand for cloud data storage, social networking, and file sharing is constantly increasing. In this framework, the possibility to manipulate the magnetic order in a solid-state material on the picosecond and subpicosecond time-scale is attractive. From the scientific perspective, it is relevant that the femtosecond duration of optical and near-infrared laser pulses allows exciting magnetic media in nonequilibrium states and directly probing the relaxation dynamics. This implies a real-time observation of spin dynamics in regimes where the conventional and well-established thermodynamical description does not hold.

The regime of the light−matter interaction strongly depends on the material investigated. Visible and near-infrared laser pulses are absorbed by free electrons in metallic samples; thus the subsequent spin dynamics is strongly dominated by laser-induced heating and energy dissipations. This regime of light−spin interaction resulted in spectacular phenomena, such as the ultrafast demagnetization[75−77] and the all-optical picosecond reversal of the magnetization in ferrimagnetic alloys.[78−80] The description of these processes is intrinsically complicated because the strong absorption of light by free electrons involves the interaction and energy flow among several degrees of freedoms (the electrons, the lattice, and the spins). On the other hand, dielectric materials are transparent to the electromagnetic radiation in the visible and near-infrared ranges of the spectrum. Consequently the light−matter interaction takes place in a nondissipative regime, which allows the excitation and manipulation of coherent collective spin excitations. Note that the relevance and interest of this regime are not restricted to the absence of energy dissipations, but they are also motivated by the possibility to clearly identify the pathways of the light−matter interaction, given the absence of the huge dissipations caused by free electrons.

BIRTH OF ULTRAFAST MAGNETISM AND DEMAGNETIZATION OF METALLIC FERROMAGNETS

The continouosly increasing demands for faster data processing have been fueling efforts to search for ever faster ways to control the magnetic state of matter.[81] The idea to change properties of a medium by means of light has long intrigued physicists and chemists.[82,83] This research direction became especially appealing after the development of femtosecond laser sources, which are able to generate sub-100 fs coherent light pulses, being among the shortest stimuli in contemporary experimental physics. Such a development has naturally raised questions about the laser-induced magnetization and speed limit of the optical control of magnetism. The quest for answers to these questions led to the seminal observation of subpicosecond demagnetization in ferromagnetic nickel by a 60 fs laser pulse.[75] This breakthrough initiated the field of ultrafast magnetism, a research activity that has caused no shortage of controversy in the scientific community redefining the borders of fundamental knowledge. The very first reports about a collapse of the net magnetization on a subpicosecond time-scale triggered an intense discussion about possible mechanisms, which can be responsible for angular momentum and energy transfer to spins on a time-scale much shorter than the characteristic times of any known interaction at that time.

Since the very early days of this exciting scientific journey, an explanation of this phenomenon in terms of a single theoretical framework has been elusive. Two different approaches emerged from the massive amount of experimental and theoretical work.[2] The first model, the so-called microscopic three-temperature model (M3TM), describes the ultrafast quenching of the magnetization in terms of electron−phonon-mediated spin flip scattering of thermalized electrons.[77] The second model relies on the superdiffusive spin transport of hot electrons in a nonequilibirum state.[84] Despite the profound microscopic difference in these two physical frameworks, it is intriguing to note that both approaches have been able to explain a variety of experiments. The study of homogeneous metallic films on insulator substrates proved unambiguously that the M3TM can fully account for the ultrafast demagnetization, in such a configuration in which the presence of a dielectric substrate rules out the spin currents from the discussion.[76] On the other hand, heterogeneous samples, for instance layered structures, demonstrated that spin transport cannot be neglected.[85,86] This multifaceted scenario suggests that both mechanisms play an important role within a certain extent, which is determined by the specific experimental conditions.[87] Recent attempts to solve this complicated puzzle have begun to make use of a degree of freedom so far vastly unexplored: the spatial dependence of the magnetization dynamics.

A very powerful solution to this issue consists in the development of X-ray scattering[88] and imaging[89] employing femtosecond pulses from free-electron lasers. Both techniques were used to investigate the time-resolved magnetization dynamics of a thin-film Co/Pt multilayer sample, with a labyrinth-domain pattern. The real-time imaging of the magnetization dynamics revealed an expansion of the demagnetized area simultaneous with the decrease of the order parameter. As the magnetization recovers, the demagnetized area shrinks as well. This evidence is consistent with the results of the scattering experiments, which are interpreted in

DOI: 10.1021/acsphotonics.6b00107
ACS Photonics 2016, 3, 1385−1400

terms of majority-spin currents flowing toward the boundary walls of the neighboring domains, where they become minority carriers and are trapped. Although the use of X-ray techniques revealed undoubtedly that the ultrafast demagnetization has a nonlocal character, it is not possible to identify in an unambiguous way the microscopic mechanism.[89]

It is very important to realize that in a model system for a spin current source contacted by a spin sink, as Co/Cu(001) films, the space-profile of the magnetization (along the interface normal direction) in the framework of the M3TM and of the superdiffusion model strongly differs.[90] Measuring the ultrafast light-induced dynamics of the complex MOKE, it is possible to explore the transient magnetization of the bilayer structure with depth-sensitivity. In fact the rotation of the polarization mainly probes the sample interface, while the ellipticity averages over the film, and it is sensitive also to the Co/Cu interface. The data reveal a dominating effect of superdiffusive currents in the first 200 fs, when the electronic system is in a nonequilibrium state. At later delays, once electrons have thermalized, the spin-flip events play a major role in the magnetization dynamics. This elegant approach allowed for the first time disentangling different contributions (spin-polarized currents and spin-flip events) to the ultrafast demagnetization, proving that in heterogeneous structures both mechanisms are relevant.

A radically different approach to the investigation of the ultrafast demagnetization process on the subwavelength regime consists in employing magnetic metallic nanoparticles. This may be relevant in terms of application perspective, given the possibility to tune the size and the shape of the particles. Moreover these studies could also reveal new pathways of the ultrafast magnetization dynamics, because the size of the system is comparable to or even smaller than the characteristic diffusion length of spin-polarized currents. Nanoparticles of Fe_3O_4 and Co revealed demagnetization times comparable with thin films, but much longer recovery time (several hundreds of picoseconds).[91−94]

In this framework, we would like to point out an interesting experiment,[95] addressing the issue of the energy efficiency of the demagentization process. Hybrid nanoparticles of Co and Ag were produced in a TiO_2 matrix with different concentrations of Ag, which resulted in different sizes of the Co particles. In particular, the highest concentration of Ag allowed obtaining Co nanoparticles with a diameter of 4.4 ± 0.1 nm. This scheme is aimed at exploiting the localized surface plasmon resonance (LSPR) of Ag particles, which can amplify the electric field of an incident light beam provided that the photon energy is resonant with the LSPR.

In these conditions, a pump fluence as low as 0.06 mJ/cm^2 (i.e., 2 orders of magnitude lower than the typical values) could reduce the magnetization by 1%, as shown by the transient ellipticity detected in the Faraday geometry.[95] More remarkably, the recovery dynamics takes place on two time-scales, a short one (2 ps) and a longer one (10 ps). This is in striking contrast with the previous observations in homogeneous magnetic nanoparticles,[91−94] in which a fast recovery has never been reported. Although a complete and conclusive discussion of the ultrafast demagnetization in hybrid nanoparticles is still missing, a scenario has been suggested.[95] The electronic excitations in the Ag nanoparticles are expected to thermalize in less than 50 fs,[95] so that the Co nanoparticles have an additional channel for ultrafast energy and heat dissipation in comparison with homogeneous nanoparticles. This process was indicated as the origin of the fast recovery dynamics.

The study of ultrafast magnetization dynamics in nanoparticles is still in its infancy, but it has the potential to reveal novel transient magnetic states on the nanoscale. The possibility to combine different elements in hybrid nanoparticles and to control the size and geometry of the resultant structure provides a novel playground to explore the nanometer and subwavelength regime. Note that in this case interactions among the nanoparticles can be neglected, since they are isolated in the insulating TiO_2 matrix. Therefore, the magnetization dynamics can turn out to be qualitatively and quantitatively different than in nanometer-scale domains in thin films. Not only are topological objects, like domain walls, totally absent in nanoparticles, but also macroscopic and collective concepts commonly employed in thin films and bulk materials (e.g., magnons, lattice, electron−phonon coupling) are not straightforwardly applicable to these systems and should be redefined.

The ultrafast demagnetization of metallic ferromagnets shows the feasibility to quench the macroscopic magnetic order on the femtosecond time-scale. However, it does not answer a fundamental question regarding the possibility to arbitrarily manipulate the macroscopic magnetization in an ultrafast fashion. Whether femtosecond laser pulses can also initiate the magnetization reversal is the next question discussed in this review.

■ ULTRAFAST ALL-OPTICAL SWITCHING IN METALLIC ALLOYS

The discovery of the all-optical helicity-dependent switching (AOS) of the magnetization fueled even further the activity in the ultrafast magnetism research field. It was demonstrated that a 40 fs circularly polarized laser pulse can reverse the magnetization of a ferrimagnetic amorphous GdFeCo alloy in the absence of any magnetic field.[78] Soon after this discovery, it was realized that the AOS proceeds along yet unexplored routes, via a strongly nonequilibrium state with no net magnetization of the Fe-sublattice.[79] The first proposed mechanism of all-optical switching was inspired by the discovery of the femtosecond inverse Faraday effect in dielectric materials.[4] It was suggested that the AOS in GdFeCo occurs as a result of a twofold effect of light. First, due to the spin−orbit interaction, an excitation of electrons by means of circularly polarized light can be represented as an effective magnetic field acting on electronic spins. Second, the laser pulse causes ultrafast demagnetization, bringing the magnet into a state with no net magnetization and high magnetic susceptibility so that even a weak magnetic field can reverse the order parameter. Although computational studies[96] have confirmed the feasibility of such a scenario, they clearly showed that a light-induced effective magnetic field of 20 T is required to be present in the medium, on a much longer time-scale than the duration of the laser pulses. A new understanding of the all-optical switching in GdFeCo alloys was achieved with the help of X-ray spectroscopy with femtosecond temporal resolution. It was shown that femtosecond laser excitation of GdFeCo triggers demagnetization of the Gd- and Fe-sublattice at two different time-scales.[80] Therefore, the optical stimulus perturbs the medium, inducing a strongly nonequilibrium state, from which the relaxation dynamics is accompanied by the reversal of the net magnetization. Theoretical descriptions of this spectacular phenomenon concluded that the optically induced magnet-

DOI: 10.1021/acsphotonics.6b00107
ACS Photonics 2016, 3, 1385−1400

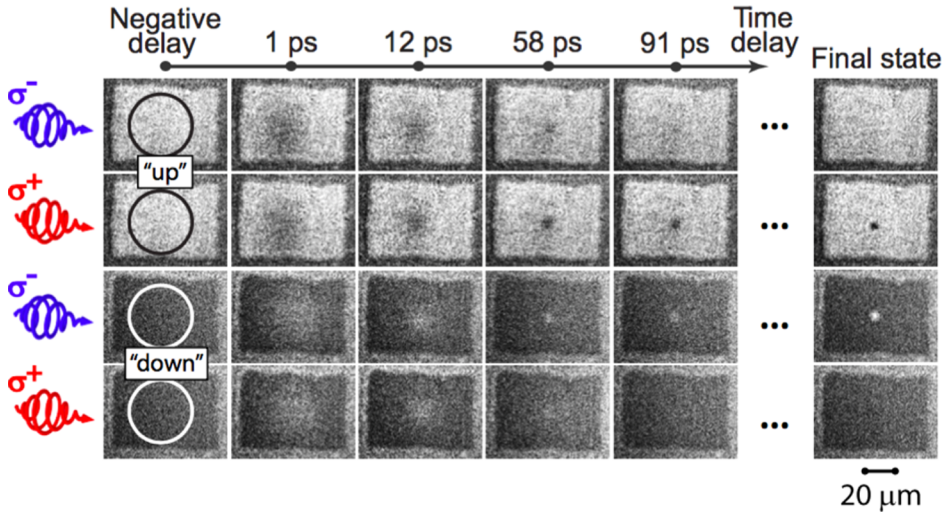

Figure 7. Magnetization evolution in $Gd_{24}Fe_{66.5}Co_{9.5}$ after excitation with σ^+ and σ^- circularly polarized pulses at room temperature. The domain is initially magnetized up (white domain) and down (black domain). The last column shows the final state of the domains after a few seconds. The circles show areas actually affected by pump pulses.

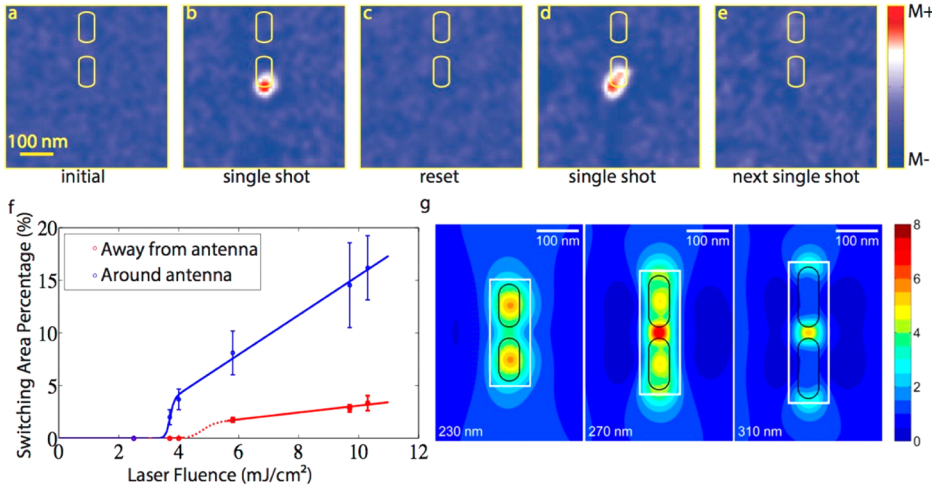

Figure 8. Antenna-mediated switching is reproducible and reversible. (a) Initial magnetic contrast around the selected antenna after being magnetic saturated in a field of 1.6 T. The gold scale bar is 100 nm in length. (b) Magnetic contrast after first laser pulse of 3.7 mJ/cm^2. A small domain of 53.4 nm is switched. (c) The magnetization is reset again using an external magnetic field. (d) Magnetic contrast after the first laser pulse of 4.0 mJ/cm^2 on the newly saturated sample. A domain of comparable size as shown in (b) is switched in the same region. (e) Magnetic contrast after a second laser pulse of 4.0 mJ/cm^2. The magnetization of the region switched in (d) is toggled back to its original state. (f) Blue data show the laser fluence-dependent switched sample area within 100 × 250 nm, 100 × 290 nm, and 100 × 330 nm regions around the 230, 290, and 310 nm Au antennas, respectively. Red data show the switched area in regions without any near-field enhancement. Above 3.7 mJ/cm^2 incident fluence, all optical switching in the vicinity of the antennas is observed. Above 5.8 mJ/cm^2 incident fluence, switching is observed in multiple locations away from the antennas. In both regions, a linear increase in the switched area is observed with increasing laser fluence above an onset threshold. (g) Calculated near-field enhancement around the three antenna lengths overlaid with white boxes to illustrate the "around antenna" regions defined above.

ization reversal relies on ultrafast heating and can even be induced by linearly polarized light.[97,98] In this scenario the helicity-dependent absorption (i.e., magnetic circular dichroism) is the origin of the helicity-dependent switching[99] shown in Figure 7.

From the point of view of the magnetic recording, the AOS can become a realistic path to pursue if the size of the domain switched becomes comparable with a 50 nm size, which is typically achieved in heat-assisted magnetic recording. The size of the smallest domain recorded with the help of AOS was approximately 5 μm. An attempt to localize the AOS on a nanometer scale was made by sample patterning.[100−102] This approach allowed reducing the size of the switched area down to 200 nm. In TbFeCo it is possible to switch domains as small as 300 nm, by focusing light with a confocal microscope.[103] It was suggested that plasmonic structures could reduce the size of the optically recorded magnetic domain, given a design able to confine femtosecond circularly polarized laser pulses well below the diffraction limit.[104] Experimental realization of helicity-dependent AOS at the nanoscale has been a challenge so far. However, realizing that the ultrafast magnetic recording can be induced even by linearly polarized light allowed us to significantly simplify the design of the antennas.

In ref 105 gold two-wire antennas were placed on a TbFeCo film. These structures are resonant with the optical field, which is enhanced in the near-field by the antennas. Using X-ray

DOI: 10.1021/acsphotonics.6b00107
ACS Photonics 2016, 3, 1385−1400

imaging techniques for magnetic domains, it was demonstrated that a single femtosecond optical laser pulse is able to reverse magnetization in the areas where field enhancement is expected to occur (see Figure 8). The minimum fluence required to switch areas close to the antennas is lower (3.7 mJ/cm^2) than in the other regions of the sample (5.8 mJ/cm^2). Despite the reproducibility of the AOS, the position and the size of the switched area cannot be controlled. This is ascribed to the inhomogeneous structure of TbFeCo, revealed by SEM images.[105] By exploiting the field-confining capability of the plasmonic nanoantennas, reproducible AOS was observed in domains with a lateral size of 53 nm, as requested in terms of data recording applications. A noncontact geometry also is required to make this a viable alternative technology; this could be achieved using the present two-wire antenna structure atop a flattened atomic force microscopy tip.[106]

It is worth discussing the attempts to control the magnetization in microstructures without any plasmonic antennas, since they led to unexpected results. Employing magnetization-sensitive microscopy techniques, the light-induced spin dynamics of patterned samples of rare-earth transition metal alloys was addressed.[102] Different microstructures have been realized in a GdFeCo thin film. Strong effects of light interference within these structures resulted in an enhanced energy absorption for smaller areas. Micropatterned samples showed a strong decrease in the energy requirements for optically induced magnetization changes. It was also suggested that it should be possible to optically switch structures with a 20 × 20 nm^2 size employing techniques such as near-field optics and, especially, plasmonic antennas to confine the impinging pulses of energy as low as 10 fJ per bit. Another example of interference in microstructures during AOS was reported.[101] Finite-difference time domain methods were employed to simulate the laser absorption profile within the magnetic structure. The feasibility of a nanoscale magnetic switching was revealed, even for the case of an unfocused incoming laser beam. This effect was explained as a result of coupling and propagation of the laser pulse within the magnetic structure, where it experiences a complex combination of refraction and interference. All these processes result in focusing of the pulse energy onto a localized region of the structure. In the simulations it was found that the effect persists down to structural sizes of 5 × 5 nm^2. In the same work, subwavelength AOS was observed with sub-100 ps temporal resolution. Such time-resolved studies were performed in microstructure with sizes down to 1 × 1 μm^2 with the help of photoemission electron microscopy and X-ray magnetic circular dichroism. An all-optical investigation of the AOS in a GdFeCo film with femtosecond time- and micrometer space-resolution revealed only a localized response.[107] Achieving the nanometer-resolution, while retaining the femtosecond time-resolution, is therefore a very important development of the AOS investigation. It is thus clear that the transition from continuous to nanostructured materials has greatly enriched the physics of both magneto-optics and femtosecond optomagnetism. Plasmonic effects allow an enhancement of the magneto-optical signals and result in highly efficient all-optical magnetic recording at the nanoscale. It is believed that further developments of magneto-optics and optomagnetism in nanostructured and, in particular, in plasmonic materials can eventually facilitate studies of the physics of magnetism with both nanometer and femtosecond resolution. Once such techniques are available, one would be able to study magnetism at the length- and time-scale of the exchange interaction, one of the strongest quantum phenomena, which is ultimately responsible for the very existence of magnetic order. These developments could also be highly relevant for magnonics, which is believed to be able to substitute electronics as a novel technology for data processing. Studies of magnetic dynamics with both femtosecond temporal and nanometer spatial resolution would allow to push the operational frequency of future nanomagnonic devices to the unprecedentedly fast THz domain. Interestingly, methods to investigate femtosecond nanomagnonics are already available nowadays, as discussed in the following part of this review.

FEMTONANOMAGNONICS

The word magnonics describes the field of science that investigates the transfer and process of information by spin waves.[108] This activity is motivated by the high technological potential of magnons as carriers of data in next-generation devices, due to several peculiar features of the magnetic eigenmodes. First of all, using a vector (spin wave) instead of a scalar (charge) allows the already ongoing development of computational algorithms that employ the additional degree of freedom (phase).[108,109] Elements of spin wave computing and logic have already been demonstrated.[109] Second, spin waves offer high flexibility, since the operational frequency of devices could span the GHz and THz ranges. This property bolsters even further the natural possibility to integrate magnonic with electronic and photonic technologies, given the existence of electrical and optical schemes to excite and detect spin waves.[109,110] Third, a magnon-based computational scheme could be straightforwardly scaled down to the nanometer size, since the wavelength of magnons can be as short as 1 nm. Most importantly, the basic concept of magnonics does not involve any motion of electrons, avoiding any Joule heating and opening the door to the utilization of insulators.[108]

The experimental demonstration of light-induced coherent spin excitations in a dielectric material on the femtosecond time-scale broadened the horizons of the ultrafast magnetism research area,[2,4] suggesting even the possibility of a femtosecond all-optical approach to magnonics. This significant breakthrough revealed a pathway of ultrafast coherent spin manipulation that does not involve the excitation of hot electrons, unlike the processes investigated in metals. Consequently, these findings ignited a surge of interest toward dielectric materials, since they allow an ultrafast access and manipulation of the spin degree of freedom that does not require energy dissipations.

In this framework, the main mechanism of spin excitation is light scattering of magnons by femtosecond laser pulses, i.e., impulsive stimulated Raman scattering (ISRS).[4,111−113] In particular, in a nondissipative regime, the interaction between light and the magnetic system can be written using the following Hamiltonian:[114]

$$\hat{H} = \sum_{\lambda,\nu} \epsilon^{\lambda\nu}(\hat{S}) E^{\lambda} E^{\nu} \tag{5}$$

where $\epsilon^{\lambda\nu}$ is the dielectric tensor which depends on the spin ($\hat{S}$), while the greek letters are indexes and E is the electric field of light. The tensor $\epsilon^{\lambda\nu}$ can be expanded in powers of the spin operators. Following a well-established approach,[114,115] we may express the spin-dependent components of $\epsilon^{\lambda,\nu}$ as

DOI: 10.1021/acsphotonics.6b00107
ACS Photonics 2016, 3, 1385−1400

$$\epsilon^{\lambda\nu} = \sum_i \sum_\gamma K^{\lambda\nu\gamma} \langle \hat{S}_i^{\gamma} \rangle + \sum_i \sum_{\gamma\delta} G^{\lambda\nu\gamma\delta} \langle \hat{S}_i^{\gamma} \rangle \langle \hat{S}_i^{\delta} \rangle + \sum_{i,j} \sum_{\gamma\delta} \rho^{\lambda\nu\gamma\delta} \langle \hat{S}_i^{\gamma\uparrow} \hat{S}_j^{\delta\downarrow} \rangle \quad (6)$$

where *i,j* represent ionic sites and higher order terms are omitted. Each term in this expansion represents a Raman mode. As it is well established, this expansion of the dielectric tensor can be employed also to describe the action of a magnetic material on a light beam, given the intimate connection between the tensors defining the Raman scattering on magnons and the magneto-optical coefficients.[114,116] For this reason, the Raman scattering on magnons can be properly defined as *optomagnetism*, being the reciprocal effect of magneto-optics. The first two terms of eq 6 are connected with the lowest energy magnetic excitations, correspondent to a single spin-flip process, the so-called one-magnon modes. These spin waves have wavevectors close to the center of the Brillouin zone. Note that although the second term is quadratic in the spin, it describes a single magnon excitation. In fact this term is linear in the spin deviation, i.e., in the spin transversal component, which represents the generation of a single magnon.[114] It was demonstrated that a light beam can induce these low-energy magnons via a modification of the spin−orbit coupling.[114,117] Therefore, the only requirement, as far as the material is concerned, is a nonvanishing spin−orbit coupling in the excited state. Note that this allows the observation of the optomagnetic effect in an impressive variety of systems, with different magnetic structures (canted antiferromagnets, ferrimagnets, compensated antiferromagnets, conical antiferromagnets).[2,112,113,118,119] More importantly, the ISRS excitation of coherent magnons was experimentally achieved even in a regime in which the laser pulses did not release any energy into the lattice.[120] Choosing the proper pump-photon energy, it was demonstrated that a regime of spin dynamics void of any signature of heated electrons and phonons is realized. This was called zero-absorption regime.[120]

The use of magnons in dielectric materials for data transfer and processing devices has been recently discussed in view of the progress achieved in the magnonics research area. Necessary requirements are the generation, control, and detection of magnons. Moreover, it has been pointed out that magnons have the potential to achieve the THz regime in terms of clock frequency of future magnon-based computational devices.[108] The high frequency implies also a short wavelength, which would allow the miniaturization of the technology. The optical stimulus represents an intriguing alternative to the more traditional schemes, involving a microwave resonant excitation and electrical detection of spin waves.

Recently a concept of selective excitation and detection of different magnon modes has been demonstrated. The information contained in the polarization eigenstate of a fully polarized pump beam was transferred into the magnetic eigenmodes of a three-sublattice antiferromagnet in a one-to-one fashion. The information was then converted back from the magnetic system to the polarization state of a probe beam, once again in a one-to-one process. This write-read cycle was claimed to be the proof of concept of the feasibility to employ laser pulses as a stimulus in magnonics, the so-called optomagnonics.[121]

However, the wavelength of the magnons excited in this work lies in the micrometer scale, and, as far as the frequency of the spin waves is concerned, the THz regime is barely achieved. Note that this is a direct consequence of accessing magnons at the center of the Brillouin zone, which have the shortest wavevector and lowest frequency. This has been considered an intrinsic disadvantage of the optical approach, since the wavevector of light seems to restrict the excitation of spins to magnons with a wavevector close to 0. More generally, the idea of a manipulation of the magnetic order on a sub-100 nm scale by means of visible electromagnetic radiation has been hitherto believed highly unlikely, if not impossible.

However, the magnon dispersion of a cubic antiferromagnet indicates that in principle such a limitation could be overcome by accessing magnons near the edges of the Brillouin zone. The dispersion curve can be calculated following a conventional procedure,[122] considering the spin deviations (i.e., spin flips generating the spin waves or magnons) from the fully aligned antiferromagnetic ground state. Figure 9 reveals that these spin

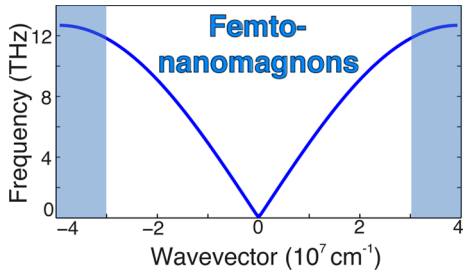

Figure 9. Spin wave dispersion of the Heisenberg antiferromagnet $KNiF_3$. The magnons close to the edges of the Brillouin zone (blue area) have a femtosecond period and a nanometer wavelength; thus they are called femto-nanomagnons. Note that the frequency of such spin waves is defined mostly by the exchange interaction.

waves for the Heisenberg antiferromagnet $KNiF_3$ have a period on the femtosecond time-scale and a wavelength on the order of 1 nm. Despite the absence of an ultrafast stimulus matching simultaneously the frequency and the wavevector of such magnons, it is possible to access this region of the dispersion via the Raman effect.[114,117,123,124] A light beam can effectively flip two spins belonging to different sublattices (see Figure 10a), by triggering in this way two magnons. Such an excitation leaves the total spin unchanged and equal to zero, and the wavevector is conserved as well, provided that the wavevectors of the two magnons have equal amplitude and opposite orientation. This bound state of two magnons, called a two-magnon (2M) mode, can be excited via a Raman process, and it is described by the last term of the expansion reported in eq 6. The Raman spectrum of $KNiF_3$ reveals that the period of the 2M mode is approximately 45 fs; therefore laser pulses with a duration of 10 fs are required for an ISRS excitation. The dynamics of the 2M mode can be measured via the time evolution of a second-order magneto-optical effect, also described by the last term of eq 6, consisting in the dynamics of the correlation function between two nearest neighbor spins.[115]

The data in Figure 10b reveal oscillations at the frequency of 22 THz and lifetime of 500 fs. The temperature dependence of the effect confirmed that this signal corresponds to the 2M mode, indicating that coherent magnons with a 45 fs period and a wavelength of 1 nm were excited and probed.[122] An analytical model of the spin dynamics was formulated in the approximation of free magnons. In this theoretical framework the detected time dependence of the spin correlation function

DOI: 10.1021/acsphotonics.6b00107
ACS Photonics 2016, 3, 1385−1400

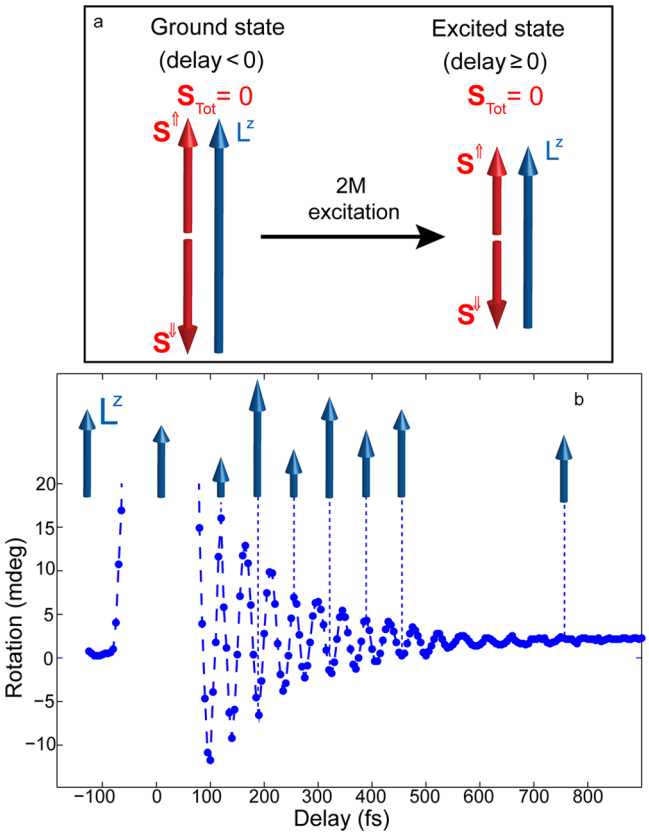

Figure 10. (a) The two-magnon excitation is equivalent to a spin-flip event per sublattice. Thus, the magnetization of each sublattice ($S^{\uparrow}$ and $S^{\downarrow}$, represented by the two red arrows with opposite orientation) and, therefore, the antiferromagnetic vector (L^z, blue arrow) is decreased in the excited state. The sum of the spins of the two sublattices, and thus the total magnetization, vanishes both in the ground and in the excited state. (b) The transient rotation of the probe polarization was measured with the electric fields of the pump and the probe beams linearly polarized along the z- and x-axes, respectively. The pump fluence was set to ∼8.6 mJ cm^{-2}. The corresponding dynamics of L^z (blue arrows) is schematically represented. When the pump pulses impinge on the sample (0 delay), L^z decreases, due to the generation of magnons. At positive delays, oscillations at the frequency of the 2M mode are visible.

coincides with the time dependence of the antiferromagnetic vector, which is the order parameter. Therefore, it was concluded that the oscillations in Figure 10b correspond to coherent longitudinal dynamics of the antiferromagnetic vector.

The phase and the amplitude of the short-wavelength magnons were coherently manipulated by changing the excitation conditions (see Figure 11). More specifically, rotating the polarization of the pump beam by 90° results in the reversal of the sign of the signal, i.e., a π-shift of the phase of the magnons. Aiming at controlling also the amplitude of the oscillations, a double-pump excitation scheme was developed. When the two pump pulses were shifted in time by a delay equal to the period of the 2M mode, the amplitude of the oscillations was enhanced. On the other hand, by setting the delay equal to half-period of the 2M mode, the signal was quenched. Consequently, a coherent manipulation of the order parameter in an antiferromagnet has been achieved on the 10 fs time-scale.

The approach employed to trigger and detect spin excitations with nanometer wavelength is very general and can be applied to several material classes. It is important to underline that the ISRS excitation of the two-magnon mode allows the manipulation of the spin system on a subwavelength regime without any energy dissipations. The wavelength of the pump beam was the same employed to disclose the zero-absorption regime in the same material.[120,122] These results bring the optomagnonics concept to the femtosecond time- and nanometer length-scale simultaneously, disclosing the novel regime named *femto-nanomagnonics*.

CONCLUSIONS

Here we have presented the current situation in the area of plasmonics conjugated with magneto-optics and femtosecond optomagnetism. The main stress in magnetoplasmonics was put on the structures having three important features. Namely, they are (i) plasmonic, (ii) periodically nanostructured, and (iii) magnetic. Having the aim to identify how the first two features affect the magneto-optical properties of the structure, particular attention was paid to the question of whether they can be used to enhance the magneto-optical effects. This has been accomplished exemplarily by addressing several main magneto-optical effects such as the transverse Kerr effect, the Faraday effect, and even the magneto-optical transmission effect. Thus, numerical calculations showed that the TMOKE for bare iron garnet film is very small, $\delta \propto 10^{-4}$, both for transmitted and reflected light. When the film is covered by a smooth gold layer, the TMOKE is resonantly enhanced up to $\delta \propto 5 \times 10^{-3}$, but it can be observed only in reflection while the transmission almost vanishes. If the second feature—nanostructuring—comes into play, extraordinary optical transmission appears with a giant TMOKE δ reaching 1.5×10^{-2}. A similar resonant increase is also demonstrated for the other magneto-optical effects.

Such an enhancement makes magnetic plasmonic crystals very promising for applications in ultra-high-sensitivity devices, such as magnetic field sensors[125] and optical data processing.

The second part of the review summarized a reciprocal problem, being focused on the most relevant progress in the area of ultrafast optical control of magnetism on the nanoscale. A new physical arena has just been disclosed, in which phenomena defying the established understanding of magnetism are expected to be observed. Note that the novel regime of combined femtosecond time- and nanometer length-scale invalidates some concepts conventionally accepted in solid-state physics, such as the continuous medium approximation. On the other hand, inducing all-optical switching in TbFeCo in the 50 nm range made this concept a more realistic technological option, as the length-scale of interest is now comparable to the heat-assisted magnetic recording. The femto-nanomagnonics regime demonstrated in a dielectric material can lay the foundations for magnon-based devices operating in the 20 THz regime and directly scalable to the nanometer size. It should not be overlooked that no energy dissipations are required at all, nor occurred, in this novel regime of spin dynamics. An enhancement of the optomagnetic effect in a plasmonic crystal has already been shown theoretically.[126] Recent progress in the femtosecond control of the magnetization in conjunction with the concept of a plasmonic crystal opens the possibility for modulation of light intensity and polarization in plasmonic crystals on the ultrafast time-scale.

DOI: 10.1021/acsphotonics.6b00107
ACS Photonics 2016, 3, 1385−1400

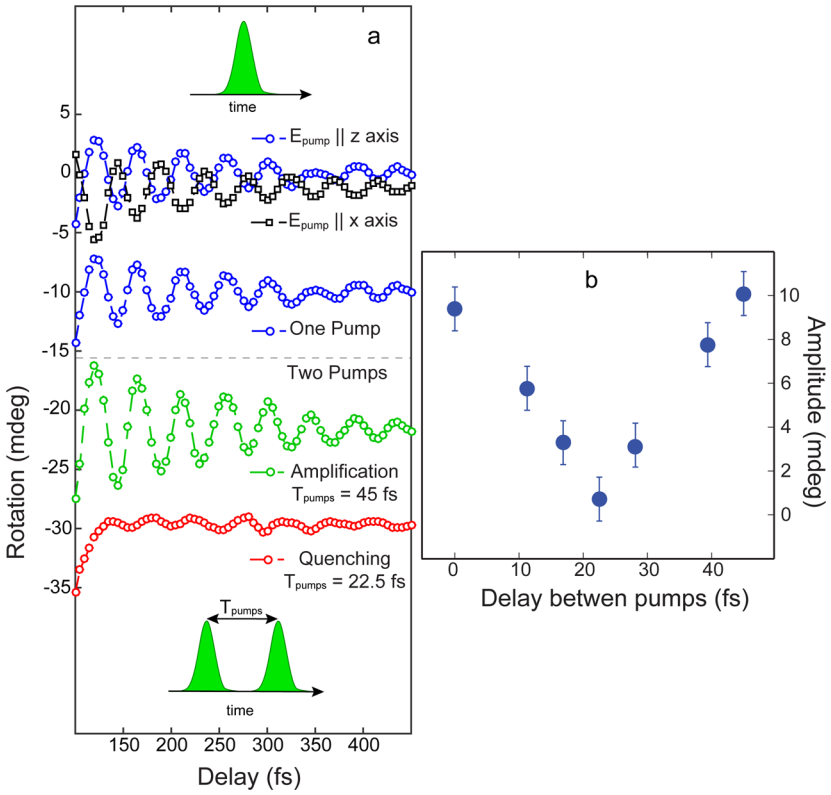

Figure 11. (a) The blue- and black-dotted traces were obtained using a single pump beam linearly polarized along the *z*-axis (blue circles) and the *x*-axis (black squares). The phase of the oscillations is shifted by π. The single-pump measurement is repeated for the sake of comparison with the results of the double-pump experiments. The green-circle data set was observed by delaying two pump pulses by T_{pumps} = 45 fs, i.e., the period of the two-magnon mode. The coherent amplification of the signal is observed. The coherent oscillations were quenched when the delay between the two pump pulses was set to T_{pumps} = 22.5 fs. The fluence of both pump beams was set to ~1.5 mJ cm^{-2}. The temperature was 80 K. The probe beam was polarized along the *x*-axis. (b) Amplitude of the first oscillation as a function of the delay between the two pumps (T_{pumps}); the periodic trend is clear. The error bars are defined as twice the sensitivity of our setup.

AUTHOR INFORMATION

Corresponding Author

*E-mail (D. Bossini): davide@gono.phys.s.u-tokyo.ac.jp.

Notes

The authors declare no competing financial interest.

ACKNOWLEDGMENTS

The work was supported by the Russian Science Foundation (Grant No. 14-32-00010) in the review and analysis of the magnetoplasmonics part, de Nederlandse Organisatie voor Wetenschappelijk Onderzoek (NWO), de Stichting voor Fundamenteel Onderzoek der Materie (FOM), and the program "Leading Scientist" of the Russian Ministry of Education of Science (14.Z50.31.0034) in the review of the opto-magnetism part.

REFERENCES

(1) Zvezdin, A.; Kotov, V. *Modern Magneetooptics and Magnetooptical Materials*; IOP: Bristol, 1997.

(2) Kirilyuk, A.; Kimel, A.; Rasing, T. Ultrafast Optical Manipulation of Magnetic Order. *Rev. Mod. Phys.* **2010**, *82*, 2731−2784.

(3) Kimel, A.; Kirilyuk, A.; Rasing, T. Femtosecond opto-magnetism: ultrafast laser manipulation of magnetic materials. *Laser Photonics Rev.* **2007**, *1*, 275−287.

(4) Kimel, A. V.; Kirilyuk, A.; Usachev, P. A.; Pisarev, R. V.; Balbashov, A. M.; Rasing, T. Ultrafast non-thermal control of magnetization by istantaneous photomagnetic pulses. *Nature* **2005**, *435*, 655−657.

(5) De Jong, J. A.; Razdolski, I.; Kalashnikova, A. M.; Pisarev, R. V.; Balbashov, A. M.; Kirilyuk, A.; Rasing, T.; Kimel, A. V. Coherent Control of the Route of an Ultrafast Magnetic Phase Transition via Low-amplitude Spin Precession, *Phys. Rev. Lett.* **2012**, *108*.10.1103/PhysRevLett.108.157601

(6) Afanasiev, D.; Kimel, A. V.; Pisarev, R. V.; Kirilyuk, A.; Ivanov, B. A.; Afanasiev, D.; Ivanov, B. A.; Rasing, T. Control of the Ultrafast Photoinduced Magnetization across the Morin point in $DyFeO_3$. *Phys. Rev. Lett.* **2016**, *116*, 097401.

(7) Challener, W. A.; Itagi, A. V. In *Near-Field Optics for Heat-Assisted Magnetic Recording (Experiment, Theory, and Modeling)*; Schlesinger, M., Ed.; Springer: New York, 2009; pp 53−111.

(8) Sarychev, A.; Shalaev, V. *Electrodynamics of Metamaterials*; World Scientific: Singapore, 2007.

(9) Inoue, M.; Arai, K.; Fujii, T.; Abe, M. One-dimensional magnetophotonic crystals. *J. Appl. Phys.* **1999**, *85*, 5768.

(10) Levy, M.; Yang, H.; Steel, M.; Fujita, J. Flat-top response in one-dimensional magnetic photonic bandgap structures with Faraday rotation enhancement. *J. Lightwave Technol.* **2001**, *19*, 1964.

(11) Zvezdin, A.; Belotelov, V. Magnetooptical properties of two dimensional photonic crystals. *Eur. Phys. J. B* **2004**, *37*, 479.

(12) Kuz'michev, A.; Kreilkamp, L.; Nur-E-Alam, M.; Bezus, E.; Vasiliev, M.; Akimov, I.; Alameh, K.; Bayer, M.; Belotelov, V. Tunable Optical Nanocavity of Iron-garnet with a Buried Metal Layer. *Materials* **2015**, *8*, 3012−3023.

(13) Maier, S. *Plasmonics: Fundamentals and Applications*; Springer: New York, 2007.

(14) Ozbay, E. Plasmonics: Merging Photonics and Electronics at Nanoscale Dimensions. *Science* **2006**, *311*, 189.

(15) Bozhevolnyi, S. I. *Plasmonic Nanoguides and Circuits*; Pan Stanford Publ: Singapore, 2008.

DOI: 10.1021/acsphotonics.6b00107
ACS Photonics 2016, 3, 1385−1400

(16) Pohl, M.; Belotelov, V.; Akimov, I.; Kasture, S.; Vengurlekar, A.; Gopal, A.; Zvezdin, A.; Yakovlev, D.; Bayer, M. Plasmonic crystals for ultrafast nanophotonics: Optical switching of surface plasmon polaritons. *Phys. Rev. B: Condens. Matter Mater. Phys.* **2012**, *85*, 081401.
(17) Voigt, W. *Magneto und Elektrooptic*; B.G. Teubner: Leipzig, 1908.
(18) Ferguson, P. E.; Stafsudd, O. M.; Wallis, R. F. Surface magnetoplasma waves in nickel. *Physica B+C* **1977**, *86-88*, 1403.
(19) Burke, J.; Stegeman, G.; Tamir, T. Surface-polariton-like waves guided by thin, lossy metal films. *Phys. Rev. B: Condens. Matter Mater. Phys.* **1986**, *33*, 5186.
(20) Hickernell, R.; Sarid, D. Long-range surface magnetoplasmons in thin nickel films. *Opt. Lett.* **1987**, *12*, 570.
(21) Aers, G.; Boardman, A. The theory of semiconductor magnetoplasmon-polariton surface modes: Voigt geometry. *J. Phys. C: Solid State Phys.* **1978**, *11*, 945.
(22) Kushwaha, M. Plasmons and magnetoplasmons in semiconductor heterostructures. *Surf. Sci. Rep.* **2001**, *41*, 1.
(23) Torrado, J.; Gonzalez-Diaz, J.; Gonzalez, M.; Garcia-Martin, A.; Armelles, G. Magneto-optical effects in interacting localized and propagating surface plasmon modes. *Opt. Express* **2010**, *18*, 15635.
(24) Murzina, T.; Kolmychek, I.; Nikulin, A.; Gan'shina, E.; Aksipetrov, O. Plasmonic and magnetic effects accompanying optical second-harmonic generation in Au/Co/Au nanodisks. *JETP Lett.* **2009**, *90*, 504.
(25) Kolmychek, I.; Murzina, T.; Aksipetov, O. Nonlinear magneto-optical transversal Kerr effect in magneto-plasmonic nanosandwiches. *Proc. SPIE* **2009**, 739434.
(26) Temnov, V. V.; Armelles, G.; Woggon, U.; Guzatov, D.; Cebollada, A.; Garcia-Martin, A.; Garcia-Martin, J.-M.; Thomay, T.; Leitenstorfer, A.; Bratschitsch, R. Active magneto-plasmonics in hybrid metal?ferromagnet structures. *Nat. Photonics* **2010**, *4*, 107−111.
(27) González-Díaz, J. B.; García-Martín, A.; Armelles, G.; García-Martín, J. M.; Clavero, C.; Cebollada, A.; Lukaszew, R.; Skuza, J.; Kumah, D.; Clarke, R. Surface-magnetoplasmon nonreciprocity effects in noble-metal/ferromagnetic heterostructures. *Phys. Rev. B: Condens. Matter Mater. Phys.* **2007**, *76*, 153402.
(28) Vila, E. F.; Bendana Sueiro, X. M.; González-Díaz, J. B.; García-Martín, A.; García-Martín, J. M.; Cebollada Navarro, A.; Armelles Reig, G.; Meneses Rodriguez, D.; Sandoval, E. M. Surface plasmon resonance effects in the magneto-optical activity of Ag?Co?Ag trilayers. *IEEE Trans. Magn.* **2008**, *44*, 3303−3306.
(29) Temnov, V. V. Ultrafast acousto-magneto-plasmonics. *Nat. Photonics* **2012**, *6*, 728−736.
(30) Martín-Becerra, D.; González-Díaz, J. B.; Temnov, V. V.; Cebollada, A.; Armelles, G.; Thomay, T.; Leitenstorfer, A.; Bratschitsch, R.; García-Martín, A.; González, M. U. Enhancement of the magnetic modulation of surface plasmon polaritons in Au/Co/Au films, *Appl. Phys. Lett.* **2010**, *97*.18311410.1063/1.3512874
(31) Martín-Becerra, D.; Temnov, V. V.; Thomay, T.; Leitenstorfer, A.; Bratschitsch, R.; Armelles, G.; García-Martín, A.; González, M. U. Spectral dependence of the magnetic modulation of surface plasmon polaritons in noble/ferromagnetic/noble metal films. *Phys. Rev. B: Condens. Matter Mater. Phys.* **2012**, *86*, 035118.
(32) Caballero, B.; García-Martín, A.; Cuevas, J. C. Hybrid Magnetoplasmonic Crystals Boost the Performance of Nanohole Arrays as Plasmonic Sensors. *ACS Photonics* **2016**, *3*, 203−208.
(33) Kekesi, R.; Martín-Becerra, D.; Meneses-Rodríguez, D.; García-Pérez, F.; Cebollada, A.; Armelles, G. Enhanced nonreciprocal effects in magnetoplasmonic systems supporting simultaneously localized and propagating plasmons. *Opt. Express* **2015**, *23*, 8128−8133.
(34) Grunin, A.; Zhdanov, A.; Ezhov, A.; Ganshina, E.; Fedyanin, A. Surface-plasmon-induced enhancement of magneto-optical Kerr effect in all-nickel subwavelength nanogratings. *Appl. Phys. Lett.* **2010**, *97*, 261908.
(35) Newman, D.; Wears, M.; Matelon, R.; Hooper, I. Magneto-optic behaviour in the presence of surface plasmons. *J. Phys.: Condens. Matter* **2008**, *20*, 345230.
(36) Clavero, C.; Yang, K.; Skuza, J.; Lukaszew, R. Magnetic-field modulation of surface plasmon polaritons on gratings. *Opt. Lett.* **2010**, *35*, 1557−1559.
(37) Armelles, G.; Cebollada, A.; García-Martín, A.; García-Martín, J. M.; González, M.; González-Díaz, J. B.; Ferreiro-Vila, E.; Torrado, J. Magnetoplasmonic nanostructures: systems supporting both plasmonic and magnetic properties. *J. Opt. A: Pure Appl. Opt.* **2009**, *11*, 114023.
(38) Razdolski, I.; Makarov, D.; Schmidt, O. G.; Kirilyuk, A.; Rasing, T.; Temnov, V. V. Nonlinear Surface Magnetoplasmonics in Kretschmann Multilayers. *ACS Photonics* **2016**, *3*, 179−183.
(39) Strelniker, Y. M.; Bergman, D. J. Transmittance and transparency of subwavelength-perforated conducting films in the presence of a magnetic field. *Phys. Rev. B: Condens. Matter Mater. Phys.* **2008**, *77*, 205113.
(40) Dubovik, V.; Tosunyan, L. Toroidal moments in the physics of electromagnetic and weak interactions. *Sov. J. Part. Nucl.* **1983**, 504.
(41) Kalish, A.; Belotelov, V.; Zvezdin, A. Optical properties of toroidal media. *Proc. SPIE* **2007**, 67283D.
(42) Gusev, N.; Belotelov, V.; Zvezdin, A. Surface plasmons in nanowires with toroidal magnetic structure. *Opt. Lett.* **2014**, *39*, 4108−4111.
(43) Davydova, M.; Dodonov, D.; Kalish, A.; Belotelov, V.; Zvezdin, A. Schrödinger plasmon?solitons in Kerr nonlinear heterostructures with magnetic manipulation. *Opt. Lett.* **2015**, *40*, 5439−5442.
(44) Belotelov, V.; Bykov, D.; Doskolovich, L. Extraordinary transmission and giant magneto-optical transverse Kerr effect in plasmonic nanostructured films. *J. Opt. Soc. Am. B* **2009**, *26*, 1594.
(45) Belotelov, V.; Bykov, V.; Doskolovich, L.; Kalish, A.; Zvezdin, A. Giant transversal Kerr effect in magneto-plasmonic heterostructures: The scattering-matrix method. *J. Exp. Theor. Phys.* **2010**, *110*, 816.
(46) Prokopov, A.; Vetoshko, P.; Shumilov, A.; Shaposhnikov, A.; Kuz'michev, A.; Koshlyakova, N.; Berzhansky, V.; Zvezdin, A.; Belotelov, V. Epitaxial Bi-Gd-Sc iron-garnet films for magnetophotonic applications. *J. Alloys Compd.* **2016**, *671*, 403.
(47) Levy, M.; Li, R. Polarization rotation enhancement and scattering mechanisms in waveguide magnetophotonic crystals. *Appl. Phys. Lett.* **2006**, *89*, 121113.
(48) Khartsev, S.; Grishin, A. High performance latching-type luminescent magneto-optical photonic crystals. *Opt. Lett.* **2011**, *36*, 2806−2808.
(49) Heinrich, B.; Burrowes, C.; Montoya, E.; Kardasz, B.; Gift, E.; Song, Y.; Sun, Y.; Wu, M. Spin Pumping at the Magnetic Insulator (YIG)/Normal Metal (Au) Interfaces. *Phys. Rev. Lett.* **2011**, *107*, 066604.
(50) Wang, Z.; Cherkasskii, M.; Kalinikos, B.; Wu, M. Observation of spin-wave dark soliton pairs in yttrium iron garnet thin films. *Phys. Rev. B: Condens. Matter Mater. Phys.* **2011**, *91*, 174418.
(51) Belotelov, V.; Akimov, I.; Pohl, M.; Kotov, V.; Kasture, V. A.; Vengurlekar, A. S.; Gopal, A.; Yakovlev, D.; Zvezdin, A.; Bayer, M. Enhanced magneto-optical effects in magnetoplasmonic crystals. *Nat. Nanotechnol.* **2011**, *6*, 370.
(52) Kreilkamp, L.; Belotelov, V.; Chin, J.; Neutzner, S.; Dregely, D.; Wehlus, T.; Akimov, I.; Bayer, M.; Strizker, B.; Giessen, H. Waveguide-Plasmon Polaritons Enhance Transverse Magneto-Optical Kerr Effect. *Phys. Rev. X* **2013**, *3*, 041019.
(53) Pohl, M.; Kreilkamp, L.; Belotelov, V.; Akimov, I.; Kalish, A.; Khokhlov, N.; Yallapragada, V.; Gopal, A.; Nur-E-Alam, M.; Vasiliev, M.; Yakovlev, D.; Alameh, K.; Zvezdin, A.; Bayer, M. Tuning of the transverse magneto-optical Kerr effect in magneto-plasmonic crystals. *New J. Phys.* **2013**, *15*, 075024.
(54) Khokhlov, N.; Prokopov, A.; Shaposhnikov, A.; Berzhansky, V.; Kozhaev, M.; Andreev, S.; Ravishankar, A.; Gopal Achanta, V.; Bykov, D.; Zvezdin, A.; Belotelov, V. Photonic crystals with plasmonic patterns: novel type of the heterostructures for enhanced magneto-optical activity. *J. Phys. D: Appl. Phys.* **2015**, *48*, 09500.
(55) Ctistis, G.; Papaioannou, E.; Patoka, P.; Gutek, J.; Fumagalli, P.; Giersig, M. Optical and Magnetic Properties of Hexagonal Arrays of

DOI: 10.1021/acsphotonics.6b00107
ACS Photonics 2016, 3, 1385−1400

Subwavelength Holes in Optically Thin Cobalt Films. *Nano Lett.* **2008**, *9*, 1−6.
(56) Caballero, B.; García-Martín, A.; Cuevas, J. C. Faraday effect in hybrid magneto-plasmonic photonic crystals. *Opt. Express* **2015**, *23*, 22238−22249.
(57) González-Díaz, J. B.; García-Martín, A.; Armelles, G.; Navas, D.; Vázquez, M.; Nielsch, K.; Wehrspohn, R. B.; Gösele, U. Enhanced Magneto-Optics and Size Effects in Ferromagnetic Nanowire Arrays. *Adv. Mater.* **2007**, *19*, 2643−2647.
(58) González-Díaz, J. B.; García-Martín, A.; García-Martín, J. M.; Cebollada, A.; Armelles, G.; Sepúlveda, B.; Alaverdyan, Y.; Käll, M. Plasmonic Au/Co/Au Nanosandwiches with Enhanced Magneto-optical Activity. *Small* **2008**, *4*, 202−205.
(59) Du, G.; Mori, T.; Saito, S.; Takahashi, M. Shape-enhanced magneto-optical activity: Degree of freedom for active plasmonics. *Phys. Rev. B: Condens. Matter Mater. Phys.* **2010**, *82*, 161403.
(60) Feng, H. Y.; Feng, L.; Meneses-Rodríguez, D.; Armelles, G.; Cebollada, A. From disk to ring: Aspect ratio control of the magnetoplasmonic response in Au/Co/Au nanostructures fabricated by hole-mask colloidal lithography. *Appl. Phys. Lett.* **2015**, *106*, 083105.
(61) Tomita, S.; Kato, T.; Tsunashima, S.; Iwata, S.; Fujii, M.; Hayashi, S. Magneto-Optical Kerr Effects of Yttrium-Iron Garnet Thin Films Incorporating Gold Nanoparticles. *Phys. Rev. Lett.* **2006**, *96*, 167402.
(62) Tkachuk, S.; Lang, G.; Krafft, C.; Rabin, O.; Mayergoyz, I. Plasmon resonance enhancement of Faraday rotation in thin garnet films. *J. Appl. Phys.* **2011**, *109*, 07B717.
(63) Fujikawa, R.; Baryshev, A.; Kim, J.; Uchida, H.; Inoue, M. Contribution of the surface plasmon resonance to optical and magneto-optical properties of a Bi:YIG-Au nanostructure. *J. Appl. Phys.* **2008**, *103*, 07D301.
(64) Uchida, H.; Masuda, Y.; Fujikawa, R.; Baryshev, A.; Inoue, M. Large enhancement of Faraday rotation by localized surface plasmon resonance in Au nanoparticles embedded in Bi:YIG film. *J. Magn. Magn. Mater.* **2009**, *321*, 843−845.
(65) Belotelov, V.; Doskolovich, L.; Kotov, V.; Bezus, E.; Bykov, D.; Zvezdin, A. Magnetooptical effects in the metal-dielectric gratings. *Opt. Commun.* **2007**, *278*, 104.
(66) Belotelov, V.; Doskolovich, L.; Kotov, V.; Bezus, E.; Bykov, D.; Zvezdin, A. Faraday effect enhancement in metal-dielectric plasmonic systems. *Proc. SPIE* **2007**, 65810S.
(67) Belotelov, V.; Zvezdin, A. Magneto-optical properties of photonic crystals. *J. Opt. Soc. Am. B* **2005**, *22*, 286−292.
(68) Chin, J.; Steinle, T.; Wehlus, T.; Dregely, D.; Weiss, T.; Belotelov, V.; Stritzker, B.; Giessen, H. Nonreciprocal plasmonics enables giant enhancement of thin-film Faraday rotation. *Nat. Commun.* **2013**, *4*, 1599.
(69) Belotelov, V. I.; Kreilkamp, L. E.; Akimov, I. A.; Kalish, A. N.; Bykov, D. A.; Kasture, S.; Yallapragada, V. J.; Gopal, A. V.; Grishin, A. M.; Kharatsev, S. I.; Nur-E-Alam, M.; Vasiliev, M.; Doscolovich, L. L.; Yakovlev, D. R.; Alameh, K.; Zvezdin, A. K.; Bayer, M. Plasmon-mediated magneto-optical transparency. *Nat. Commun.* **2013**, *4*, 2128.
(70) Belotelov, V. I.; Kreilkamp, L. E.; Akimov, I. A.; Kalish, A. N.; Bykov, D. A.; Kasture, S.; Yallapragada, V. J.; Gopal, A. V.; Grishin, A. M.; Kharatsev, S. I.; Nur-E-Alam, M.; Vasiliev, M.; Doscolovich, L. L.; Yakovlev, D. R.; Alameh, K.; Zvezdin, A. K.; Bayer, M. Magneto-photonic intensity effects in hybrid metal-dielectric structures. *Phys. Rev. B: Condens. Matter Mater. Phys.* **2014**, *89*, 045118.
(71) Kalish, A.; Ignatyeva, D.; Belotelov, V.; Kreilkamp, L.; Akimov, I.; Gopal, A.; Bayer, M.; Sukhorukov, A. Transformation of mode polarization in gyrotropic plasmonic waveguides. *Laser Phys.* **2014**, *24*, 094006.
(72) Stenning, G. B.; Bowden, G. J.; Maple, L. C.; Gregory, S. A.; Sposito, A.; Eason, R. W.; Zheludev, N. I.; de Groot, P. A. J. Magnetic control of a meta-molecule. *Opt. Express* **2013**, *21*, 1456.
(73) Cai, W.; Shalaev, V. *Optical Metamaterials: Fundamentals and Applications*; Springer, 2009.
(74) Boardman, A. D.; Hess, O.; Mitchell-Thomas, R. C.; Rapoport, Y. G.; Velasco, L. Temporal solitons in magnetooptic and metamaterial waveguides. *Photonics and Nanostructures - Fundamentals and Applications* **2010**, *8*, 228.
(75) Beaurepaire, E.; Merle, J. C.; Daunois, A.; Bigot, J. Y. Ultrafast spin dynamics in ferromagnetic nickel. *Phys. Rev. Lett.* **1996**, *76*, 4250−4253.
(76) Schellekens, A. J.; Verhoeven, W.; Vader, T. N.; Koopmans, B. Investigating the contribution of superdiffusive transport to ultrafast demagnetization of ferromagnetic thin films. *Appl. Phys. Lett.* **2013**, *102*, 252408.
(77) Koopmans, B.; Malinowski, G.; Dalla Longa, F.; Steiauf, D.; Fähnle, M.; Roth, T.; Cinchetti, M.; Aeschlimann, M. Explaining the paradoxical diversity of ultrafast laser-induced demagnetization. *Nat. Mater.* **2010**, *9*, 259−65.
(78) Stanciu, C. D.; Hansteen, F.; Kimel, A. V.; Kirilyuk, A.; Tsukamoto, A.; Itoh, A.; Rasing, T. All-Optical Magnetic Recording with Circularly Polarized Light. *Phys. Rev. Lett.* **2007**, *99*, 047601.
(79) Vahaplar, K.; Kalashnikova, A. M.; Kimel, A. V.; Hinzke, D.; Nowak, U.; Chantrell, R.; Tsukamoto, A.; Itoh, A.; Kirilyuk, A.; Rasing, T. Ultrafast Path for Optical Magnetization Reversal via a Strongly Nonequilibrium State. *Phys. Rev. Lett.* **2009**, *103*, 117201.
(80) Radu, I.; Vahaplar, K.; Stamm, C.; Kachel, T.; Pontius, N.; Dürr, H. A.; Ostler, T. A.; Barker, J.; Evans, R. F. L.; Chantrell, R. W.; Tsukamoto, A.; Itoh, A.; Kirilyuk, A.; Rasing, T.; Kimel, A. V. Transient ferromagnetic-like state mediating ultrafast reversal of antiferromagnetically coupled spins. *Nature* **2011**, *472*, 205−8.
(81) Stohr, J.; Siegmann, H. C. *Magnetism From Fundamentals to Nanoscale Dynamics*; Springer, 2006.
(82) Kovalenko, V. F.; Nagaev, É. L. Photoinduced magnetism. *Soviet Physics Uspekhi* **1986**, *29*, 297−321.
(83) EVANS, D. F. Photomagnetism of Triplet States of Organic Molecules. *Nature* **1955**, *176*, 777−778.
(84) Battiato, M.; Carva, K.; Oppeneer, P. M. Superdiffusive Spin Transport as a Mechanism of Ultrafast Demagnetization. *Phys. Rev. Lett.* **2010**, *105*, 027203.
(85) Malinowski, G.; DallaLonga, F.; Rietjens, J. H. H.; Paluskar, P. V.; Huijink, R.; Swagten, H. J. M.; Koopmans, B. Control of speed and efficiency of ultrafast demagnetization by direct transfer of spin angular momentum. *Nat. Phys.* **2008**, *4*, 855−858.
(86) Melnikov, A.; Razdolski, I.; Wehling, T. O.; Papaioannou, E. T.; Roddatis, V.; Fumagalli, P.; Aktsipetrov, O.; Lichtenstein, A. I.; Bovensiepen, U. Ultrafast Transport of Laser-Excited Spin-Polarized Carriers in Au/Fe/MgO(001). *Phys. Rev. Lett.* **2011**, *107*, 076601.
(87) Turgut, E.; La-o Vorakiat, C.; Shaw, J. M.; Grychtol, P.; Nembach, H. T.; Rudolf, D.; Adam, R.; Aeschlimann, M.; Schneider, C. M.; Silva, T. J.; Murnane, M. M.; Kapteyn, H. C.; Mathias, S. Controlling the Competition between Optically Induced Ultrafast Spin-Flip Scattering and Spin Transport in Magnetic Multilayers. *Phys. Rev. Lett.* **2013**, *110*, 197201.
(88) Pfau, B.; Schaffert, S.; Müller, L.; Gutt, C.; Al-Shemmary, A.; Büttner, F.; Delaunay, R.; Düsterer, S.; Flewett, S.; Frömter, R.; Geilhufe, J.; Guehrs, E.; Günther, C. M.; Hawaldar, R.; Hille, M.; Jaouen, N.; Kobs, K.; Li, K.; Mohanty, J.; Redlin, H.; Schlotter, W. F.; Stickler, D.; Treusch, R.; Vodungbo, B.; Kläui, M.; Oepen, H. P.; Lüning, J.; Grübel, G.; Eisebitt, S. Ultrafast Optical Demagnetization manipulates nanoscale spin structure in domain walls. *Nat. Commun.* **2012**, *3*, 1100.
(89) von Korff Schmising, C.; Pfau, B.; Schneider, M.; Günther, C. M.; Giovannella, M.; Perron, J.; Vodungbo, B.; Müller, L.; Capotondi, F.; Pedersoli, E.; Mahne, N.; Lüning, J.; Eisebitt, S. Imaging Ultrafast Demagnetization Dynamics after a Spatially Localized Optical Excitation. *Phys. Rev. Lett.* **2014**, *112*, 217203.
(90) Wieczorek, J.; Eschenlohr, A.; Weidtmann, B.; Rösner, M.; Bergeard, N.; Tarasevitch, A.; Wehling, T. O.; Bovensiepen, U. Separation of ultrafast spin currents and spin-flip scattering in Co/Cu(001) driven by femtosecond laser excitation employing the complex magneto-optical Kerr effect. *Phys. Rev. B: Condens. Matter Mater. Phys.* **2015**, *92*, 174410.

DOI: 10.1021/acsphotonics.6b00107
ACS Photonics 2016, 3, 1385−1400

(91) Hsia, C.-H.; Chen, T.-Y.; Son, D. H. Size-Dependent Ultrafast Magnetization Dynamics in Iron Oxide (Fe 3O 4) Nanocrystals. *Nano Lett.* **2008**, *8*, 571−6.
(92) Hsia, C.-H.; Chen, T.-Y.; Son, D. H. Time-Resolved Study of Surface Spin Effect on Spin?Lattice Relaxation in Fe 3O 4Nanocrystals. *J. Am. Chem. Soc.* **2009**, *131*, 9146−7.
(93) Chen, T.-Y.; Hsia, C.-H.; Chen, H.-Y.; Son, D. H. Size Effect on Chemical Tuning of Spin?Lattice Relaxation Dynamics in Superparamagnetic Nanocrystals. *J. Phys. Chem. C* **2010**, *114*, 9713−9719.
(94) Andrade, L. H. F.; Laraoui, A.; Vomir, M.; Muller, D.; Stoquert, J.-P.; Estournès, C.; Beaurepaire, E.; Bigot, J.-Y. Real Space Trajectory of the Ultrafast Magnetization Dynamics in Ferromagnetic Metals. *Phys. Rev. Lett.* **2006**, *97*, 127401.
(95) Ikemiya, K.; Konishi, K.; Fujii, E.; Kogure, T.; Kuwata-Gonokami, M.; Hasegawa, T. Self-assembly and plasmon-enhanced ultrafast magnetization of Ag?Co hybrid nanoparticles. *Opt. Mater. Express* **2014**, *4*, 1564.
(96) Vahaplar, K.; Kalashnikova, A. M.; Kimel, A. V.; Gerlach, S.; Hinzke, D.; Nowak, U.; Chantrell, R.; Tsukamoto, A.; Itoh, A.; Kirilyuk, A.; Rasing, T. All-optical magnetization reversal by circularly polarized laser pulses: Experiment and multiscale modeling. *Phys. Rev. B: Condens. Matter Mater. Phys.* **2012**, *85*, 104402.
(97) Ostler, T. A.; Barker, J.; Evans, R. F. L.; Chantrell, R. W.; Atxitia, U.; Chubykalo-Fesenko, O.; El Moussaoui, S.; Le Guyader, L.; Mengotti, E.; Heyderman, L. J.; Nolting, F.; Tsukamoto, A.; Itoh, A.; Afanasiev, D.; Ivanov, B. A.; Kalashnikova, A. M.; Vahaplar, K.; Mentink, J.; Kirilyuk, A.; Rasing, Th.; Kimel, A. V. Ultrafast heating as a sufficient stimulus for magnetization reversal in a ferrimagnet. *Nat. Commun.* **2012**, *3*, 666.
(98) Mentink, J. H.; Hellsvik, J.; Afanasiev, D. V.; Ivanov, B. A.; Kirilyuk, A.; Kimel, A. V.; Eriksson, O.; Katsnelson, M. I.; Rasing, T. Ultrafast Spin Dynamics in Multisublattice Magnets. *Phys. Rev. Lett.* **2012**, *108*, 057202.
(99) Khorsand, A. R.; Savoini, M.; Kirilyuk, A.; Kimel, A. V.; Tsukamoto, A.; Itoh, A.; Rasing, T. Role of Magnetic Circular Dichroism in All-Optical Magnetic Recording, *Phys. Rev. Lett.* **2012**, *108*.10.1103/PhysRevLett.108.127205
(100) Le Guyader, L.; El Moussaoui, S.; Buzzi, M.; Chopdekar, R. V.; Heyderman, L. J.; Tsukamoto, A.; Itoh, A.; Kirilyuk, A.; Rasing, T.; Kimel, A. V.; Nolting, F. Demonstration of laser induced magnetization reversal in GdFeCo nanostructures. *Appl. Phys. Lett.* **2012**, *101*, 022410.
(101) Le Guyader, L.; Savoini, M.; El Moussaoui, S.; Buzzi, M.; Tsukamoto, A.; Itoh, A.; Kirilyuk, A.; Rasing, T.; Kimel, A. V.; Nolting, F. Nanoscale sub-100 ps all-optical magnetization switching in GdFeCo microstructures. *Nat. Commun.* **2015**, *6*, 5839.
(102) Savoini, M.; Medapalli, R.; Koene, B.; Khorsand, A. R.; LeGuyader, L.; Duò, L.; Finazzi, M.; Tsukamoto, A.; Itoh, A.; Nolting, F.; Kirilyuk, A.; Kimel, A. V.; Rasing, T. Highly efficient all-optical switching of magnetization in GdFeCo microstructures by interference-enhanced absorption of light. *Phys. Rev. B: Condens. Matter Mater. Phys.* **2012**, *86*, 140404.
(103) Finazzi, M.; Savoini, M.; Khorsand, A. R.; Tsukamoto, A.; Itoh, A.; Duò, L.; Kirilyuk, A.; Rasing, T.; Ezawa, M. Laser-Induced Magnetic Nanostructures with Tunable Topological Properties. *Phys. Rev. Lett.* **2013**, *110*, 177205.
(104) Koene, B.; Savoini, M.; Kimel, A. V.; Kirilyuk, A.; Rasing, T. Optical energy optimization at the nanoscale by near-field interference. *Appl. Phys. Lett.* **2012**, *101*, 013115.
(105) Liu, T.-M.; Wang, T.; Reid, A. H.; Savoini, M.; Wu, X.; Koene, B.; Granitzka, P.; Graves, C.; Higley, D. J.; Chen, Z.; Razinskas, G.; Hantschmann, M.; Scherz, A.; Stöhr, J.; Tsukamoto, A.; Hecht, B.; Kimel, A. V.; Kirilyuk, A.; Rasing, Th.; Dürr, H. A. Nanoscale Confinement of All-Optical Magnetic Switching in TbFeCo - Competition with Nanoscale Heterogeneity. *Nano Lett.* **2015**, *15*, 6862−8.
(106) Farahani, J. N.; Eisler, H.-J.; Pohl, D. W.; Pavius, M.; Flückiger, P.; Gasser, P.; Hecht, B. Bow-tie optical antenna probes for single-emitter scanning near-field optical microscopy. *Nanotechnology* **2007**, *18*, 125506.
(107) Hashimoto, Y.; Khorsand, A. R.; Savoini, M.; Koene, B.; Bossini, D.; Tsukamoto, A.; Itoh, A.; Ohtsuka, Y.; Aoshima, K.; Kimel, A. V.; Kirilyuk, A.; Rasing, T. Ultrafast time-resolved magneto-optical imaging of all-optical switching in GdFeCo with femtosecond time-resolution and a ?m spatial-resolution. *Rev. Sci. Instrum.* **2014**, *85*, 063702.
(108) Chumak, A. V.; Vasyuchka, V. I.; Serga, A. A.; Hillebrands, B. Magnon spintronics. *Nat. Phys.* **2015**, *11*, 453−461.
(109) Lenk, B.; Ulrichs, H.; Garbs, F.; Münzenberg, M. The building blocks of magnonics. *Phys. Rep.* **2011**, *507*, 107−136.
(110) Kruglyak, V. V.; Demokritov, S. O.; Grundler, D. Magnonics. *J. Phys. D: Appl. Phys.* **2010**, *43*, 264001.
(111) Yan, Y.-X.; Gamble, E. B.; Nelson, K. A. Impulsive stimulated scattering: General importance in femtosecond laser pulse interactions with matter, and spectroscopic applications. *J. Chem. Phys.* **1985**, *83*, 5391.
(112) Kalashnikova, A.; Kimel, A.; Pisarev, R.; Gridnev, V.; Kirilyuk, A.; Rasing, T. Impulsive Generation of Coherent Magnons by Linearly Polarized Light in the Easy-Plane Antiferromagnet FeBO3. *Phys. Rev. Lett.* **2007**, *99*, 167205.
(113) Kalashnikova, A.; Kimel, A.; Pisarev, R.; Gridnev, V.; Usachev, P.; Kirilyuk, A.; Rasing, T. Impulsive excitation of coherent magnons and phonons by subpicosecond laser pulses in the weak ferromagnet FeBO3. *Phys. Rev. B: Condens. Matter Mater. Phys.* **2008**, *78*, 104301.
(114) Cottam, M. G.; Lockwood, D. J. *Light Scattering in Magnetic Solids*, 1st ed.; Wiley: New York, 1986.
(115) Ferre, J.; Gehring, G. A. Linear optical birefringence of magnetic crystals. *Rep. Prog. Phys.* **1984**, *47*, 513−611.
(116) Wettling, W.; Cottam, M. G.; Sandercock, J. R. The relation between one-magnon light scattering and the complex magneto-optic effects in YIG. *J. Phys. C: Solid State Phys.* **1975**, *8*, 211−228.
(117) Fleury, P.; Loudon, R. Scattering of Light by One- and Two-Magnon Excitations. *Phys. Rev.* **1968**, *166*, 514−530.
(118) Satoh, T.; Cho, S.-J.; Iida, R.; Shimura, T.; Kuroda, K.; Ueda, H.; Ueda, Y.; Ivanov, B.; Nori, F.; Fiebig, M. Spin Oscillations in Antiferromagnetic NiO Triggered by Circularly Polarized Light. *Phys. Rev. Lett.* **2010**, *105*, 077402.
(119) Ogawa, N.; Seki, S.; Tokura, Y. Ultrafast optical excitation of magnetic skyrmions. *Sci. Rep.* **2015**, *5*, 9552.
(120) Bossini, D.; Kalashnikova, A. M.; Pisarev, R. V.; Rasing, T.; Kimel, A. V. Controlling coherent and incoherent spin dynamics by steering the photoinduced energy flow. *Phys. Rev. B: Condens. Matter Mater. Phys.* **2014**, *89*, 060405.
(121) Satoh, T.; Iida, R.; Higuchi, T.; Fiebig, M.; Shimura, T. Writing and reading of an arbitrary optical polarization state in an antiferromagnet. *Nat. Photonics* **2014**, *9*, 25−29.
(122) Bossini, D.; Dal Conte, S.; Hashimoto, Y.; Secchi, A.; Pisarev, R. V.; Rasing, T.; Cerullo, G.; Kimel, A. V. Macrospin dynamics in antiferromagnets triggered by sub-20 fs injection of nanomagnons, *Nat. Commun.* **2016**, 7.1064510.1038/ncomms10645
(123) Chinn, S.; Zeiger, H.; O'Connor, J. Two-Magnon Raman Scattering and Exchange Interactions in Antiferromagnetic $KNiF_3$ and K_2NiF_4 and Ferrimagnetic $RbNiF_3$. *Phys. Rev. B* **1971**, *3*, 1709−1735.
(124) Balucani, U.; Tognetti, V. Theory of Two-Magnon Raman Scattering in the Ordered Region for Cubic Antiferromagnets. *Phys. Rev. B* **1973**, *8*, 4247−4257.
(125) Vetoshko, P.; Zvezdin, A.; Skirdanov, V.; Syvorotka, I.; Syvorotka, I.; Belotelov, V. The Effect of the Disk Magnetic Element Profile on the Saturation Field and Noise of a Magneto-Modulation Magnetic Field Sensor. *Tech. Phys. Lett.* **2015**, *41*, 456−459.
(126) Belotelov, V.; Bezus, E.; Doskolovich, L.; Kalish, A.; Zvezdin, A. Inverse Faraday effect in plasmonic heterostructures. *J.Phys:Conf.Ser.* **2010**, *200*, 092003.

DOI: 10.1021/acsphotonics.6b00107
ACS Photonics 2016, 3, 1385−1400